

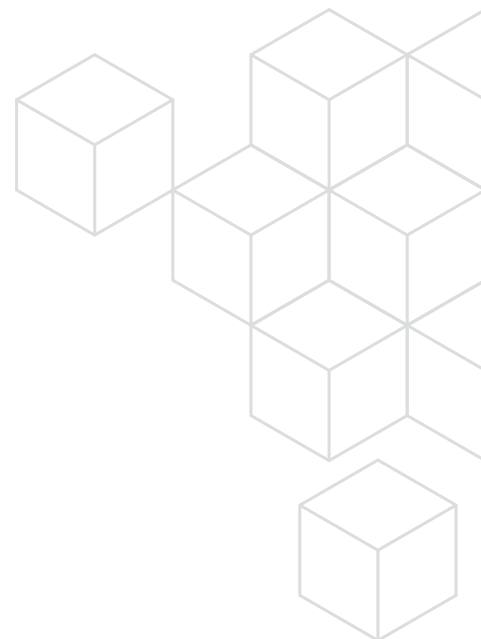
# Radar Systems

## Featuring Cadence AWR Software

Combined with advances in phased-array antennas and integration technologies, radars are moving beyond military/aerospace markets to address a host of commercial applications. This white paper showcases how the Cadence® AWR® Design Environment platform provides designers with a host of modeling and simulation technologies needed to meet the challenges of all types of radar system design.

### Contents

Overview .....	2
An Integrated Framework for Complex Radar System Design .....	3
OCW Coffee-Can Radar Optimized.....	7
Design Challenges of Next-Generation AESA Radar .....	12
MIMO/Phased-Array Antenna Systems.....	18
mmWave Automotive Radar and Antenna System Development ....	27
MACOM Designs Ka-Band MMIC Power Amplifier (Case Study) .....	36
Conclusion .....	38



## Overview

Radar applications are evolving in response to developments in semiconductor technologies, including advances in gallium nitride (GaN), silicon germanium (SiGe), and metal-oxide semiconductor (CMOS). CMOS can integrate more functionality, including digital processing and control on a single chip, providing cost and high-volume production advantages, while GaN and gallium arsenide (GaAs) still have performance advantages. Combined with advances in phased-array antennas and integration technologies, radars are moving beyond military/aerospace markets to address a host of commercial applications.



## An Integrated Framework for Complex Radar System Design

Modern radar systems are complex and depend heavily on advanced signal processing algorithms to improve their detection performance. At the same time, the radio front end must meet challenging specifications with a combination of available components, implementation technologies, regulatory constraints, requirements from the system, and signal processing. This application example showcases how AWR Design Environment® software, specifically AWR® Visual System Simulator™ (VSS) system simulation software, enables radar system architects and RF component manufacturers to design, validate, and prototype a radar system. This integrated platform provides a path for digital, RF, and system engineers to collaborate on complex radar system design.

The example project, Pulse\_Doppler\_Radar\_System.emp, illustrates key models and simulation capabilities available for practical radar design. The project and resulting measurements highlight how to configure a Pulse-Doppler radar and set up the simulation to obtain the metrics of interest for radar development. The entire pulse-Doppler (PD) radar system project includes a linear FM (LFM) chirp signal generator, RF transmitter, antennas, clutter, RF receiver, moving target detection (MTD), constant false alarm rate (CFAR) processor, and signal detector for simulation purposes.

### Theory of Operation

PD radars produce velocity data by reflecting a microwave signal from a given target and analyzing how the frequency of the returned signal has shifted due to the object’s motion. This variation in frequency provides the radial component of a target’s velocity relative to the radar. The radar determines the frequency shift by measuring the phase change that occurs in the EM pulse over a series of pulses. By measuring the Doppler rate, the radar is able to determine the relative velocity of all objects returning echoes to the radar system, whether planes, vehicles, or ground features.

As the reflector (target) moves between each transmit pulse, the returned signal has a phase difference or phase shift from pulse to pulse. This causes the reflector to produce Doppler modulation on the reflected signal. For example, assume a target at a distance R that has a radial velocity component of Vr. The round-trip distance to the target is 2R. This is equivalent to  $2R/\lambda$  wavelengths or  $(2R/\lambda)2\pi = 4\pi R/\lambda$  radians. If the  $\lambda$  phase of the transmitted signal is Equation 1, then the phase of the received signal will be:

If the  $\lambda$  phase of the transmitted signal is  $\varphi_0$ , then the phase of the received signal will be: 
$$\varphi = \varphi_0 + \frac{4\pi}{\lambda} R$$

The change in phase between pulses is 
$$\frac{d\varphi}{dt} = \frac{4\pi}{\lambda} \frac{dR}{dt} = \frac{4\pi}{\lambda} V_r$$

### System Setup

The main radar system diagram in Figure 1 includes the following building blocks: linear chirp source, RF transmitter and receiver, and the target and propagation models, as well as the receiver baseband signal processing blocks, including moving target indicator (MTI), MTD, and CFAR. User-defined parameters specifying the gain, bandwidth, and carrier frequency of both the transmitter and receiver sub-blocks can be set to values based on test specifications. A detailed look at the individual components will help explain how this DP radar works.

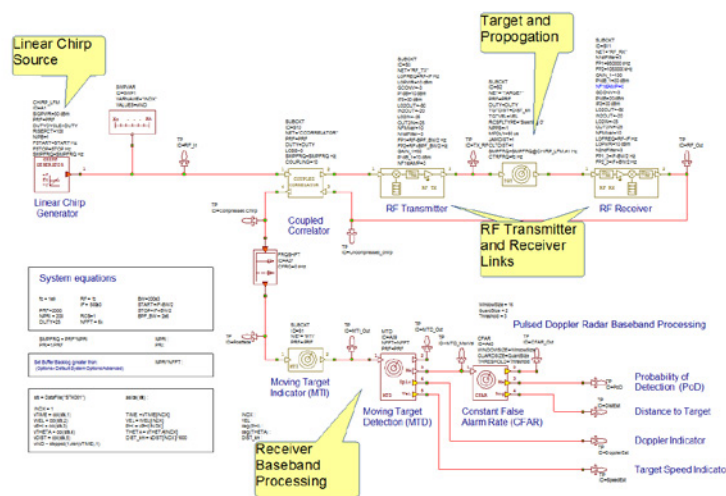


Figure 1: AWR VSS software main radar system diagram showing linear chirp source, RF transmitter and receiver links, target and propagation model, and receiver baseband signal processing blocks.

The linear chirp source (first block to the far left of the system diagram) generates a linear FM chirp signal, also known as a PD signal. The linear chirp pulse source consists of basic parameters that can be configured according to user specifications, such as pulse repetition frequency (PRF), pulse duty cycle, start/stop frequency, and sampling frequency. The pulse repetition interval (PRI) denotes the time difference between the starts of two consecutive pulses (Figure 2). The chirp duration (pulse on) is a function of duty cycle and PRI, and it is calculated as the product of the two; the duty cycle is a percentage and can take any non-negative value up to and including 100%.

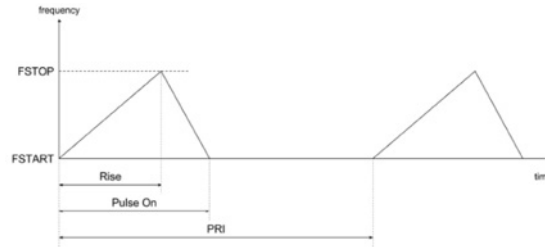


Figure 2. Control parameters defining the linear chirp generator output signal

During the active portion of the chirp, this block outputs a signal with an instantaneous frequency that changes linearly between the start and stop frequency parameters. These two parameters can have any valid frequency value, resulting in signals that can have either increasing or decreasing frequencies at the start of the chirp. Designers are also able to specify the ratio of rise and pulse on. This parameter is a percentage and can have any non-negative value up to and including 100%. The signal power during the active portion of the chirp is set by the peak power parameter of the linear chirp signal generator. A non-zero initial delay may be defined for the chirp pulse; this delay may take on any non-negative value, and a warning is generated if this delay is greater than PRI. The center frequency of the chirp signal may be user-defined. If left empty, it is set to the average of the start and stop frequencies. Similarly, the sampling frequency may also be user-defined; if left empty, it is calculated based on the global variable “\_SMPFRQ”. In this example, the chirp signal level is set to 0 dBm, PRF = 2 kHz, and DUTY = 25%.

The next block in the chain, a coupled correlator block, is commonly used for pulse compression in radar receivers. Pulse compression is a signal processing technique commonly used to increase the range resolution, as well as the signal-to-noise ratio (SNR), by modulating the transmitted pulse and then correlating the received signal with the transmitted pulse. In this example, a block performs a correlation between the signal reflected from a radar target and the transmitted signal. This requires the coupled correlator to buffer enough samples to accommodate a full PRI before it can process the chirp. To ensure a successful simulation of such scenarios, the sampling frequency should be carefully selected. The minimum value for the sampling frequency parameter would be the bandwidth of the radar signal (FSTART-FSTOP). If spectral measurements are desired, the sampling frequency can be set to a larger value. The signal next passes through the RF transmitter responsible for frequency up-conversion, filtering, and signal amplification before being radiated through the antenna toward the target. Both the RF transmitter and receiver sub-circuits define the single-stage upconverter and downconverter that are each composed of an oscillator, mixer, amplifier, and filter, as shown in Figure 3. Users may replace these subcircuits with their particular implementations.

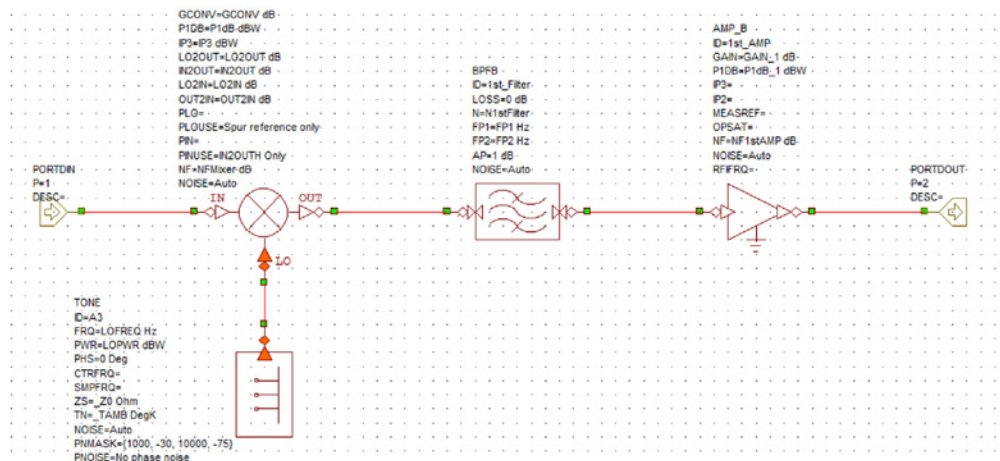


Figure 3. Components defining the RF transmitter subcircuit include an oscillator (tone source generates one or more sinusoidal tones), mixer (upconversion), filter, and amplifier

To model the entire system, this example includes a subcircuit that models the propagation channel between the transmit/receive (TX/RX) antennas, as well as the radar target. With this particular setup, users can specify the distance and relative velocity of the target and the radar cross-section (RCS) and RCS fluctuations, as well as model jammers and clutter that are often present in radar systems.

The Doppler frequency offset, target distance, and angles of arrival (THETA/PHI) are defined in a data file and vary over time. These parameters are used to define the target model. The clutter magnitude distribution is set to Rayleigh and the clutter power spectrum is formed as Weibull. The antenna radiation patterns (Figure 4) for both the transmit and receive antennas are based on file-based data from a separate EM simulation but could also have been similarly modeled with measured data. The receiver filters the incoming reflected signal prior to amplification via a low-noise amplifier (LNA), which is then downconverted through a mixer and further filtered before input into the coupled correlator. The correlator performs a correlation of the downconverted reflected signal with a coupled signal representing the input to the RF transmitter.

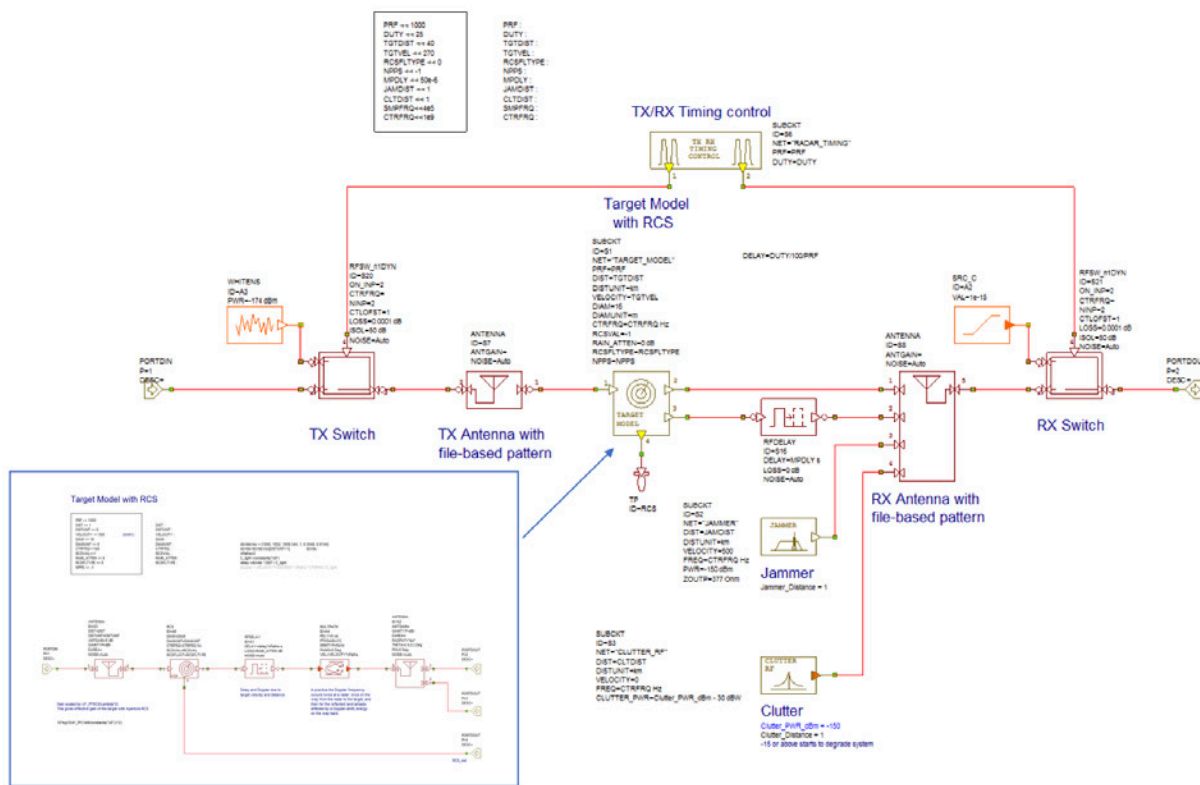


Figure 4. Subcircuit modeling both the TX and RX antennas and target model, including RCS model, multipath channel, and RF path delay

Radar searching, tracking, and other operations are usually carried out over a specified range (receive) window and defined by the difference between the radar maximum and minimum range. Reflected signals from all targets within the receive window are collected and passed through a matched filter circuitry to perform pulse compression. The correlation processor is often performed digitally using the fast Fourier transform (FFT).

To detect the moving object more effectively, MTD, which is based on a high-performance signal processing algorithm for PD radar, is used. A bank of Doppler filters or FFT operators cover all possible expected target Doppler shifts. The output of MTD is used for CFAR processing. Measurements for detection rate and false alarm rate are provided.

The MTI is used to remove stationary objects, the MTD is used to identify the remaining moving target with the FFT size set to 64, and the CFAR performs a sliding average to ensure that the detected signal is greater than a set threshold.

## Simulation Results

Under these settings, the simulation results are displayed in Figure 5. The radar signal waveform is measured in time domain at the receiver input. Because the target return signal is often blocked by clutter, jamming, and noise, detection in the time domain is not possible, and an MTD is used to perform the Doppler and range detection in the frequency domain. In the MTD model, the data are grouped for the corresponding target range and Doppler frequency. Afterward, a CFAR processor is used to set the decision threshold based on the required probabilities of detection and false alarm.

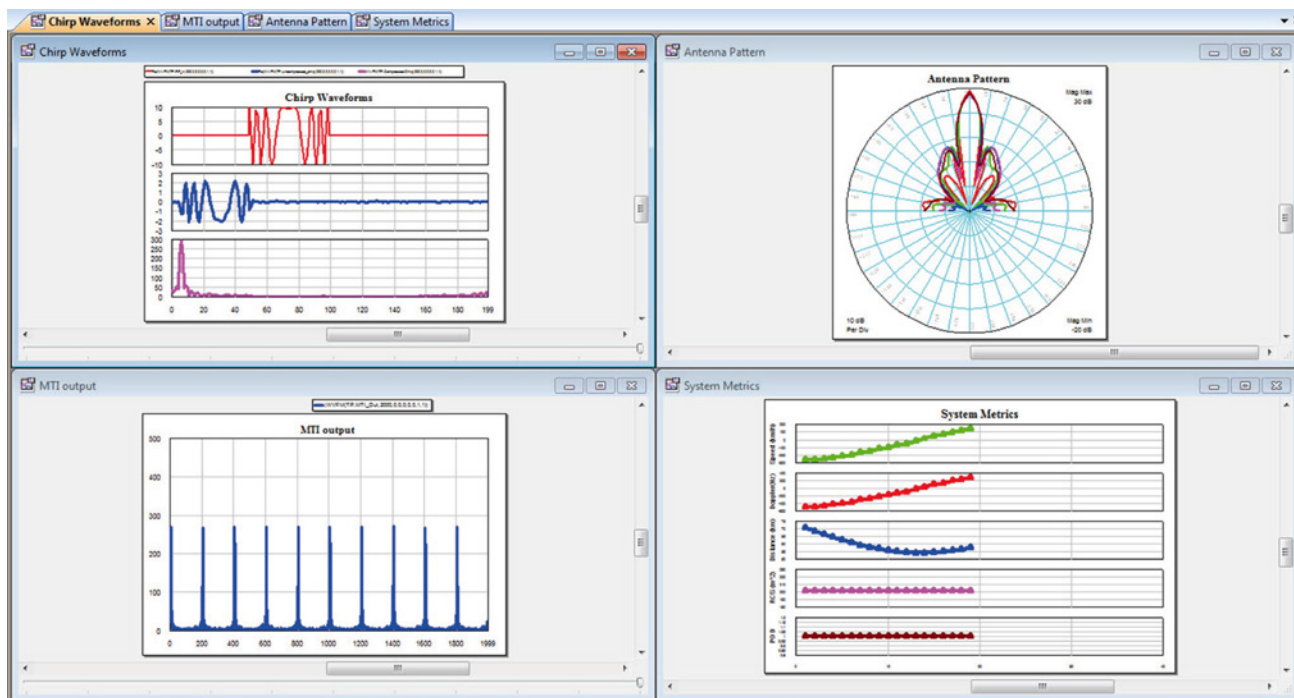


Figure 5. Plots representing various simulation results and system definitions such as antenna radiation pattern

**Chirp waveform:** The time-domain graph shows the transmitted pulse, received pulse, and the pulse after the TX/RX correlation. The correlator output is used in the baseband-received signal processing blocks to turn it into useful target information.

**Antenna pattern:** The radial plot shows the combined transmit and receive antenna pattern. When the simulation is run for the first time, the antenna parameters PHI and THETA are swept to obtain this data (see also antenna pattern VSS diagram for the swept variable setting).

**MTI output:** The time-domain plot shows the output of the MTI, which uses a second-order delay line canceler to remove effects of stationary clutter and leave Doppler information in the signal.

**System metrics (bottom right):** The graph shows the detected speed, Doppler, probability of detection (PoD), RCS, and the distance across multiple pulses.

This application example has illustrated how key models and simulation capabilities within VSS software enable practical radar design. Since much of the simulation control setup and radar system details (operating conditions) have been parameterized, this project can be used as a template for different PD applications. The radar signal is a function of PRF, power, and pulse width (duty cycle). These parameters can be modified for different cases. In the simulation, the radar signal also can be replaced by any defined signal through a data file reader in which the recorded or other custom data source can be easily used.

## OCW Coffee-Can Radar Optimized

In 2012, IEEE Spectrum published an article titled, Coffee-Can Radar: How to Build a Synthetic Aperture Imaging System with Tin Cans and AA Batteries.<sup>4</sup> This article described how to build a synthetic aperture radar using a laptop coffee-can radar system that was derived from the OpenCourseWare<sup>5</sup> (OCW) online free course materials provided through MIT. A few years later, Dr. Jim Carroll and Dr. Gent Paparisto decided to redesign the coffee-can radar system using the circuit and system design capabilities within AWR Design Environment software to “recaffeinate” the original design.

This application note describes how the original coffee-can radar system was redesigned with AWR® software, specifically AWR Microwave Office® circuit design software, AWR VSS system design software, and AWR AXIEM® and Analyst™ EM simulators, such that it delivers better performance, is less expensive to make and has a smaller footprint than the original system.

### Original OCW Design

The original coffee-can radar was based on the open ISM band at 2.4GHz, which made the parts for these Wi-Fi frequencies easily available. Connectorized Mini-Circuits components could be put together simply by fastening the connectors. The baseband signal from the radar unit was amplified and filtered using breadboard components. A laptop was used to sample the downconverted intermediate frequency (IF), and MATLAB was used for the baseband processing of the signals. The design parameters were 2.4GHz frequency with an 80MHz CW ramp waveform, less than one W of DC power, and less than one W of equivalent isotropic radiated power (EIRP).

Figure 6 shows the system diagram superimposed over the top of a photo of the actual radar system. It can be seen that the original design included a voltage-controlled oscillator (VCO), an attenuator buffer between the PA and the VCO, and a 3 dB coupler going out to the transmit antenna and the target, then coming back from the target into the receive path. The low-noise amplifier (LNA) self-mixes down from the VCO signal with the mixer. At this point, users extracted the baseband information with their laptop sound card and then performed the processing with MATLAB. The total bill of materials (BOM) cost at that time was \$360, about \$240 of which was RF circuit components. The antenna BOM (mostly cabling and connectors) was about \$54.

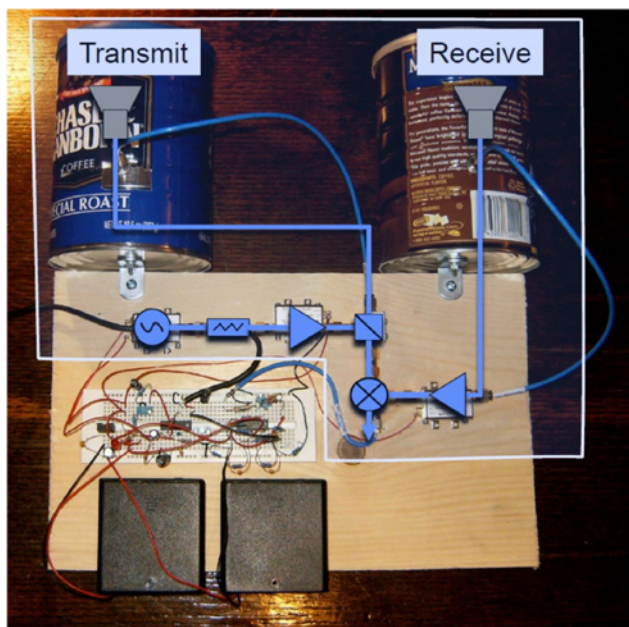


Figure 6: The original MIT OpenCourseWare coffee-can radar with connectorized components near the top and the coffee-can antennas on top of the board

4. D. Schneider, “Coffee-can Radar: How to Build a Synthetic Aperture Imaging System with Tin Cans and AA Batteries,” IEEE Spectrum, Nov. 1, 2012, <http://spectrum.ieee.org/geek-life/hands-on/coffeecan-radar>

5. G. Charvat, J. H. Williams, A. Fenn, S. Kogon, J. S. Herd, “Build a Small Radar System Capable of Sensing Range, Doppler, and Synthetic Aperture Radar Imaging,” MIT OpenCourseWare, <http://ocw.mit.edu/resources/res-ll-003-build-a-small-radar-system-capable-of-sensing-range-doppler-and-synthetic-aperture-radar-imaging-january-iap-2011/>

### The “Recaffeinated” Challenge

The recaffeinated coffee-can radar system design relied upon the simulation capabilities within AWR software in order to converge upon a final design with not only better performance but a smaller footprint and a less costly BOM.

The first step was to implement the original system as designed in the OCW material using AWR VSS software. The original system design is shown in Figure 7 with the AWR VSS radar library target model simulating the radar return. The next step then used essentially the same topology but introduced surface-mount parts, as shown in Figure 8.

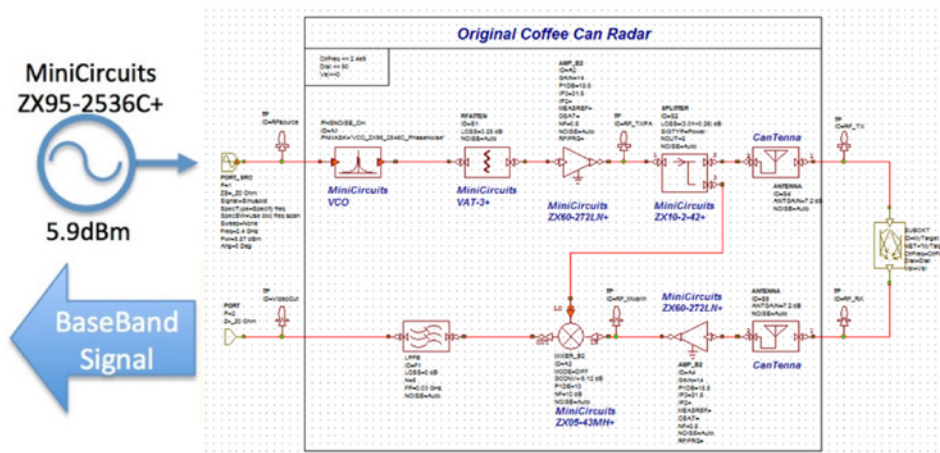


Figure 7: Original coffee-can radar implemented in AWR VSS software

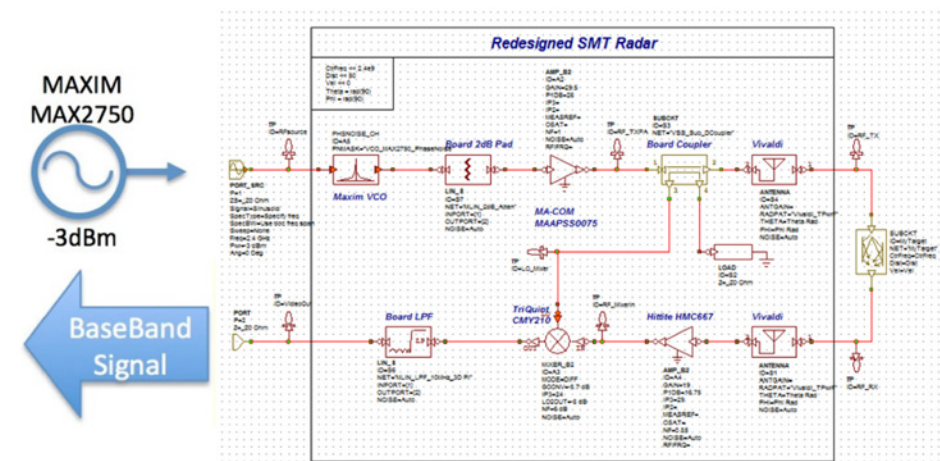


Figure 8: “Recaffeinated” coffee-can radar design in AWR VSS software using surface-mount parts

The AWR VSS simulation blocks shown in both of the above figures are mathematical models representing the performance of the actual components taken from information supplied in their datasheets. The entire block diagram has also been reimplemented representing the coffee-can antennas by gain antenna elements. All of this is mathematical in nature but can be laid out within AWR VSS software. Additionally, the AWR VSS built-in antenna radar library was used so that functions like the target model and baseband processing could be readily used.

This new design effectively replaced Mini-Circuit components with equivalent catalog surface-mount parts in the \$1-\$12 range. For other components like the attenuator and low-pass filter, surface-mount parts were also used while the 20dB coupler was implemented with microstrip on the board. Lastly, the coffee-can antennas were replaced with a planar Vivaldi antenna that was designed using AXIEM 3D planar EM software and validated in the Analyst full 3D finite element method (FEM) EM simulator. All of these efforts served to lower the BOM and footprint without sacrificing performance.

### The Details: System-Level Analysis in AWR VSS Software

The system RF budget comparison between the original system (in blue) and the recaffinated system (in red) is shown in Figure 9. The blue starts with higher output power from the VCO than the red surface-mount component, but going through the system from the VCO to the power amplifier (PA) to the 3dB coupler to the antenna, it can be seen that the redesigned system, because it uses better parts (the PA in particular), gets higher output power at the antenna. In fact, at the antenna output power, the old system is at about 20 dB EIRP, while the newer system gets about a watt, which is just at the FCC limit for a high directivity antenna like the Vivaldi.

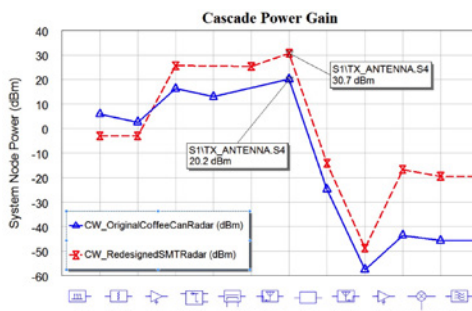


Figure 9: System budget comparison between the original and redesigned coffee-can radar

The path loss was modeled to the target and back with the AWR VSS radar library components, which also add the velocity Doppler shift if the target is moving. The received signal comes through the Vivaldi antenna, onto the LNA and the mixer. While the older system was getting about -45dBm of IF power, the new system now gets 20dBm. The RF budget calculations in Figure 4 indicate the newer system has a much higher output power at IF, which makes the target easier to detect than the original system. The graph in Figure 4 shows quantitatively how much better performance the new system achieves.

A useful feature in AWR VSS software is that once the RF system block diagrams are built, time-domain simulations can be run, and the FMCW signal can be propagated through the designed system. Figure 10 (left) shows the spectra of IF signals at the output of the old and new systems, illustrating the positive and negative frequency peaks due to the distance and Doppler shift in the FMCW radar signal. Once the IF was taken out of the simulation, FET was used to continue signal processing in the frequency domain. The locations of the two peaks were used to evaluate the target distance (range) and Doppler offset (velocity). The distance between the two peaks and how they are offset from zero determines the speed and distance. AWR VSS signal processing blocks can be used to extract these estimates. Users then get not only the spectrum but can start graphing out target distance and velocity estimates, as shown in Figure 10 (right).

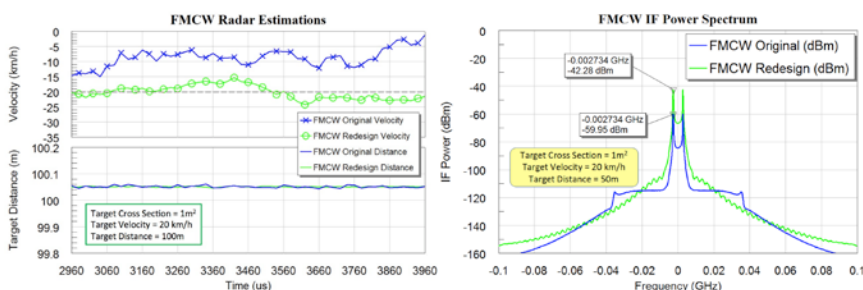


Figure 10: Time-domain FMCW spectrum simulation and measurements of target distance and velocity done with AWR VSS software

Both systems were looking at the same one-square meter target that was moving at a relative velocity of 20km/h at 100m. Both systems determined the same target distance with very little noise. The target velocity due to the Doppler shift was the more difficult measure to discriminate. In Figure 6 the redesigned system’s velocity (green) is varying about plus or minus 4km/h on a 20km/h average, or in this case -20km/h because the target was moving away from the radar system.

The original velocity (blue) is much higher in this set of time samples. If the time-domain simulation can run longer, the blue fluctuates and eventually averages out to 20km/h over a much longer time duration. What this chart highlights about the redesigned system is that it isn’t necessary to average the time-domain signal for as long a time because the new system has a much better target return on the IF path than the old system. The old system would still work, but users will have a much harder time discriminating velocity.

### The Details: PCB Design in Microwave Office and AXIEM Software

After the system diagram was finished, the surface-mount radar system was physically laid out in AWR Design Environment software (Figure 11) on a 2-layer 62mil thick FR4 board.



Figure 11: PCB design completed in AWR Design Environment software

The VCO, PA, and LNA were all produced directly from the layouts shown on the datasheets. The 1dB attenuator, the low-pass filter, and the board coupler were all designed in Microwave Office circuit design software, and the AXIEM EM simulator was used to design the coupler. The total BOM for this 3"x3" card was less than \$60 for the components going onto the board, as listed below. This was much less expensive than the original design with BOM components costing \$250.

- ▶ 23 SMT resistors
- ▶ 39 SMT caps
- ▶ 9 SMT inductors
- ▶ 3 SMA connectors
- ▶ Integrated board coupler

### The Details: Antenna Design in AXIEM and Analyst Software

As mentioned previously, the coffee-can antennas were replaced with Vivaldi planar antennas (Figure 12). Basically, there is a microstrip line coming in on the front side of the board that couples to a slot in the back. That slot then propagates out in a horn-like structure that is patterned in the backside ground, somewhat like a horn that has been squished. This is a common type of antenna in radar systems and was designed entirely in AXIEM software. The blue in the graph is the simulation, and the pink is the measurement that was done on a vector signal analyzer (VNA), which shows good agreement for the first cut. Full pattern analysis of the same structure was done with Analyst software, and this entire pattern was read into the AWR VSS diagram, enabling the designer to feed the system diagram off-boresight target location values with THETA and PHI locations. These values can also be swept in the system diagram as the target moves through the antenna pattern.

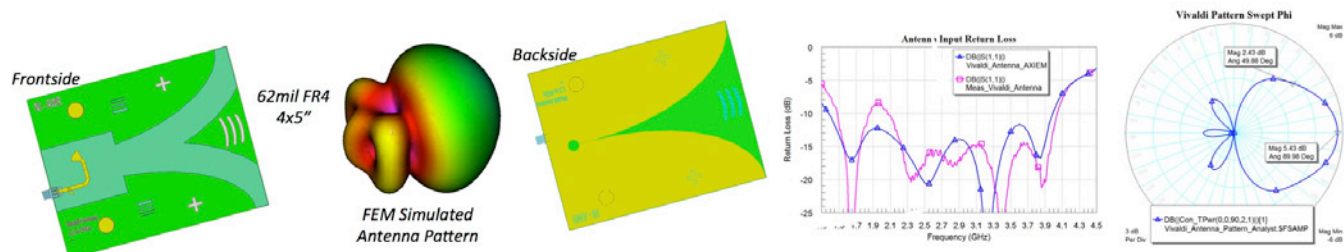


Figure 12. Vivaldi planar antennas, which replaced the original coffee-can antennas

Figure 13 is a photo of the complete system, consisting of the 3"x3" radar testbed, the Vivaldi antennas for transmit/receive, and the breadboard and power supply on the backside of the test board. The entire system fits in the palm of a hand. The antennas were designed so they could be mounted together with a pair of wooden dowels and moved apart to provide additional transmit-to-receive antenna isolation when connected to the radar testbed with coaxial cables.

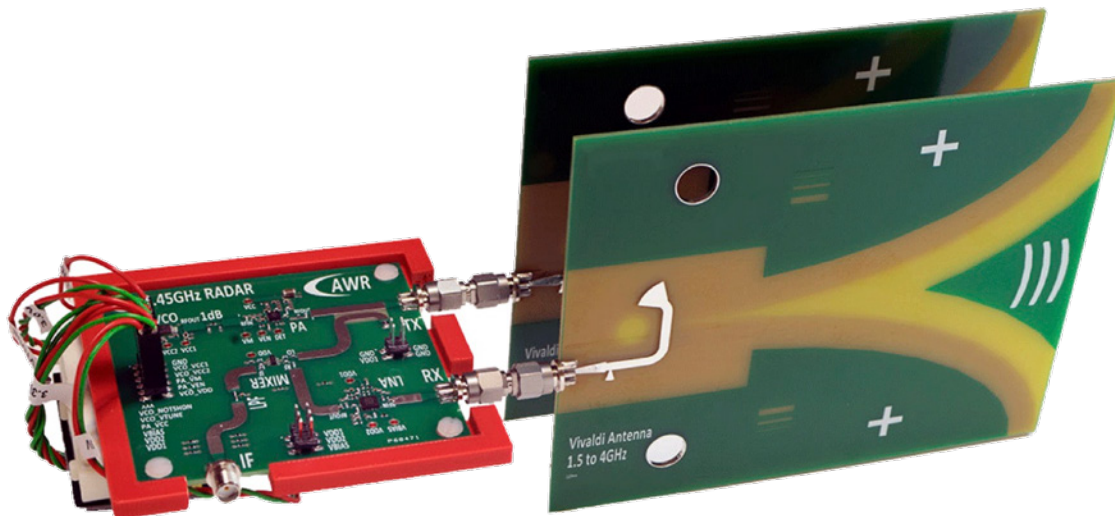


Figure 13: The entire radar RF core of the redesigned system, consisting of a 3x3 card, Vivaldi antennas, and power supply

An end-to-end FMCW radar system was fully designed in AWR Design Environment software. The recaffeinated design had better performance, was less expensive to make, and had a smaller footprint than the original coffee-can radar system.

AWR VSS software provides the ability to easily compare the system performance between the original coffee-can design and the new re-caffeinated system both for RF-link and time-domain simulations. The built-in radar library elements facilitated the building of the target model and baseband processing. A full radar test board layout was done, including EM analysis of the planar antennas, and the entire system was built and assembled. Then a co-simulation of the radar elements was run, including antennas, board coupler, attenuator, and low-pass filter, as circuit elements being done in the system simulation all at the same time.

Readers are invited to explore this design project further within AWR Design Environment software. The example project is titled "CoffeeCanRadar\_SMT\_Redesign."

## Design Challenges of Next-Generation AESA Radar

Phased-array antennas were first used in military radar systems to scan the radar beam quickly across the sky to detect planes and missiles. These systems are becoming popular for a variety of applications and new active electronically-scanned arrays (AESAs) are being used for radar systems in satellites and unmanned aerial vehicles. As these systems are deployed in new and novel ways, size and performance requirements are becoming critical and are being addressed through innovative architectures and system capabilities made possible through improvements in microwave and signal processing technologies such as GaN power amplifiers (PAs), new MMIC/Extreme MMIC devices, heterogeneous More-than-Moore integration, cost reductions for transmit/receive (T/R) modules, new mmWave silicon ICs, and electro-optic integration.<sup>6</sup>

To support these development efforts, electronic design automation (EDA) technologies are evolving to provide designers with system architecture, component specifications, physical design of individual components, and verification prior to prototyping. This white paper examines these technology trends and presents several examples where advances in AWR Design Environment software are supporting next-generation AESA and phased-array radar development.

### Phased-Array Technology

An AESA-based radar, also known as active phased-array radar (APAR), consists of individual radiating elements (antennas), each with a T/R solid-state module containing a low-noise receiver, PA, and digitally-controlled phase/delay and gain elements. Phase and amplitude control of the input signal to the individual elements provides steerable directivity of the antenna beam over both azimuth and elevation, which allows the radar to aim the main lobe of the antenna in the desired direction. Unlike a mechanically steered radar, a phased array can rotate its pattern in space with practically no delay. Digital control of the module transmit/receive gain and timing permits the design of an antenna with not only beam steering agility and interleaving radar modes, but also extremely low sidelobes, which provides a significant reduction in antenna radar signature compared to passive ESA and mechanically steered antennas.<sup>7</sup>

The width of the beam depends on the number of elements in the array. By increasing the number of elements (or sensors) in an array, the beam becomes sharper and thus more efficient in detecting smaller size targets. Today's AESA radars typically consist of thousands of individual elements electrically interconnected through increasingly complex structures designed for reduced size and weight, as well as increased performance (in other words, lower loss).

At lower RF frequencies (< 10GHz), where a longer wavelength increases the antenna size and spacing, the RF, intermediate frequency (IF), and/or baseband signal routing can be addressed with discrete components and off-the-shelf MMICs on printed circuit boards (PCBs)/packaging. The impact of longer traces will be offset by the lower PCB losses at these frequencies and the interface to the antenna can be considered independent of the IC unit cell due to the relatively flexible packaging requirements.

However, at mmWave frequencies (> 30GHz), physically short antenna spacings ( $\sim \lambda/2 < 5\text{mm}$ ), packaging losses, and manufacturing challenges with impedance-controlled multi-layer packaging interconnects make high-functionality ICs and sophisticated integration schemes more attractive. Designing these types of complex packaging schemes for high-frequency signaling must be addressed with circuit simulation and EM analysis specialized for RF and microwave electronics.<sup>8</sup>

6. <http://www.ncbi.nlm.nih.gov/pmc/articles/PMC3928903/>

7. <http://www.ausairpower.net/aesa-intro.html>

8. Xiaoxiong Gu et al., "W-Band Scalable Phased Arrays for Imaging and Communications," IEEE Commun. Mag., April 2011, pp. 196-20.

## Evolving Integration Technology

While actively-steered phased-array antennas have many advantages, they are extremely complex, and their production, especially non-recurring development costs, is significantly higher than conventional antenna design. These higher development costs are driven by the inclusion of hundreds to thousands of active electronic component modules per production unit, often implemented with custom gallium arsenide (GaAs) MMIC designs (typically five to 10 designs per system), as shown in Figure 14.

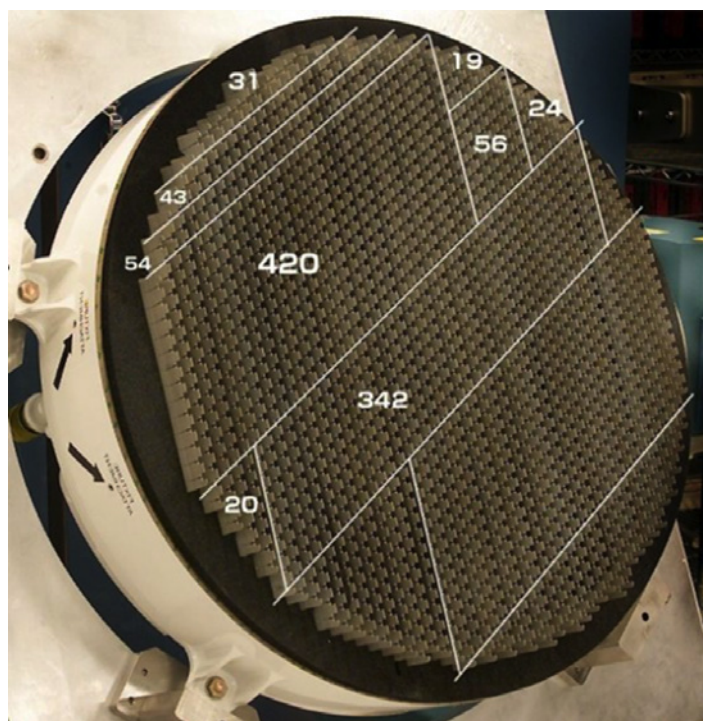


Figure 14: AN/APG-80 F-16 AESA radar from Northrup Grumman showing partial (half) count of individual array elements

Initially funded and developed through Department of Defense (DoD) support in the 1980s and 1990s, GaAs MMIC technology was the only viable option for supporting the manufacture of the densely packed (cross-section < 1cm) AESA T/R modules operating at 10-20GHz. Advances in MMIC design have been enabled by the greater availability of powerful simulation software and inexpensive compute power, which enables engineers to design increasingly complex circuits with greater accuracy and to develop libraries of frequently used RF building blocks. Where earlier MMIC development addressed the challenge of combining tens to hundreds of active and passive components, including transistors, PIN diodes, resistors, capacitors, and inductors on a single GaAs substrate, integrating AESA functionality scales in complexity by combining radio blocks such as low-noise amplifiers, PAs, switching, and phase shifters onto a single or multi-channel MMIC. Even greater functionality/density levels are being developed through multi-chip modules (MCMs) utilizing revolutionary materials, devices, and advanced integration techniques.

The Defense Advanced Research Projects Agency (DARPA) Microsystems Technology Office has two programs investigating next-generation device integration. The DARPA Compound Semiconductor Materials on Silicon (COSMOS) program focused on developing new methods to tightly integrate compound semiconductor or III-V technologies within state-of-the-art silicon CMOS circuits. The DARPA Diverse Accessible Heterogeneous Integration (DAHI) program continues this work by developing heterogeneous integration processes to intimately combine advanced III-V devices, along with emerging materials and devices, with high-density silicon CMOS technology.<sup>9</sup>

<sup>9</sup> Sanjay Raman et al., "The DARPA Diverse Accessible Heterogeneous Integration (DAHI) Program: Towards a Next-Generation Technology Platform for High-Performance Microsystems", CS MANTECH Conference, April 23rd - 26th, 2012, Boston, Massachusetts, USA

Integration technology has made significant advances over the past 10 years. In 2006, Georgia Tech Research Institute developed a four-channel X-band SiGe T/R module with the control circuitry on a single chip for the DARPA Integrated Sensor Structure (ISIS) program with a per-T/R module cost of about \$10. In 2008, researchers at the University of California San Diego (UCSD) enjoyed a huge leap in performance and integration density with the demonstration of the first RF-beamforming SiGe 6-18GHz, 8-element phased-array receiver chip with 5-bit phase control and an on-chip 8:1 combiner.<sup>10</sup> UCSD followed up this work with a demonstration of the first 16-element 45-50GHz phased-array transmitter in 2009. By 2013, a 110GHz, 4x4 wafer-scale phased-array transmitter with high-efficiency on-chip antennas was reported by UCSD,<sup>11</sup> successfully demonstrating a single chip solution, as shown in Figure 15.

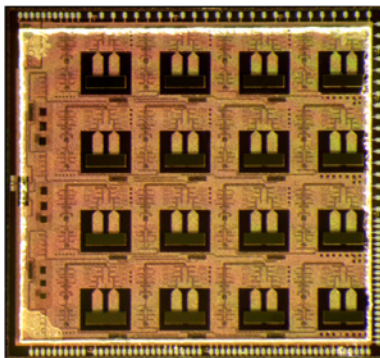


Figure 15: 4x4 wafer-scale phased-array transmitter at 110GHz

## Developments in GaN

While phased-array antennas are evolving into silicon core chips that support multiple radiating elements, preferred solutions frequently combine silicon with III-V front ends for applications that require the best possible performance, especially for figures of merit such as noise figure (NF) and output power. Increasingly, GaN is displacing GaAs as the material of choice for high-power or broadband front ends. For a fixed power level, a GaN MMIC can be one third to one quarter the size of an equivalent power GaAs MMIC, a power density that is enough to offset the higher material cost of GaN compared to GaAs. While the finished GaN wafer (including material) costs 2x that of GaAs, the resulting GaN solution is only 50-66% of the cost per RF watt generated with a GaAs solution. As the cost of GaN continues to decrease, the eventual elimination of GaAs from phased antennas could be expected for many applications.<sup>12</sup>

Continued investment in wide bandgap (WBG) semiconductors is expected to take More-than-Moore power electronics to another level. Researchers are looking to enhance GaN technology by heterogeneously integrating GaN on top of silicon wafers. The integration of GaN technology onto larger silicon wafers and the use of standard semiconductor manufacturing processing will provide significant functionality and performance advantages at a much lower cost. All these technology options require that designers have an efficient way to understand tradeoffs between individual technologies and the impact on overall performance.

Even though the density of a GaAs MMIC is much lower than that of competitive silicon digital ICs, the high-frequency electronic design requires careful attention to interconnect technology and EM-aware simulation that is able to predict the parasitic behavior that leads to performance failures. The physical arrangement or layout of components and interconnects is such a critical part of RF/microwave circuit design that AWR Design Environment utilizes a unified data model to inherently link schematic-based electrical elements to EM simulation-ready layout. This level of analysis is increasingly critical to successful MMIC development as the technology and integration levels evolve.

While the integration of III-V and silicon technologies address the size and functionality requirements of next-generation phased arrays, high-density ICs also increase the need for wafer processing quality since losing one transistor out of a hundred due to a fabrication defect amounts to losing the entire (costly) die. As a result, the design of a complete microwave RF circuit on a chip will require established RF design rules for the layout of components and interconnections. In addition, robust design by way of yield/corner analysis must also be incorporated into the design stage in order to study the impact of manufacturing tolerances.

10. <http://www.microwavejournal.com/articles/4757-an-eight-element-6-to-18-ghz-sige-bicmos-rfic-phased-array-receiver>

11. <http://phys.org/news/2012-04-silicon-wafer-scale-ghz-phased-array.html>

12. Mike Harris et al., "GaN-based Components for Transmit/Receive Modules in Active Electronically Scanned Arrays", CS MANTECH Conference, May 13th - 16th, 2013, New Orleans, Louisiana, USA

### System Simulation for Phased Arrays

Design failure and the resulting high costs of development are often due in part to the inability of high-level system tools to accurately model the interactions between the multitude of electrically interconnected channels that are specified separately. Constructing full or partial phased-array systems to investigate these unforeseen interactions is also very expensive, both in terms of the expense of fabrication and the high cost to test the interactions of hundreds to thousands of channels. This challenge will only increase as the antenna-array and beam-steering control electronics continue along the current integration path.

With the design of such systems through fabrication and test iterations being cost-prohibitive, development efforts are typically limited to one prototype in Phase I or Phase II proof-of-concept demonstration. Failure to meet the specifications would lead to an unacceptable number of design and test iterations of the complete system (antenna/electronics). Therefore, a simulation that incorporates the entire system has become a necessity. Since phased-array performance is neither driven purely by the antenna nor microwave electronics behavior, simulation must capture their combined interaction in order to accurately predict the overall system.

Often, high-level system analysis is performed using custom implementations by way of spreadsheets or generic mathematical calculations. Typically, these custom solutions vary in complexity from company to company and even between different projects within the same company. Such custom tools are generally used to specify the performance requirements of the underlying subsystems (MMICs/antennas/RF passives/control).

The more robust analysis offered by AWR VSS communication system design software combines the performance metrics of each of the subcomponents of a phased-array system to provide a more accurate accounting of the high-level system performance (Figure 16). Initially, the analysis would be used to specify the overall system component topology and performance requirements on the individual subsystems. As more detailed models of the subsystems become available, these models and/or measurements of subsystems can be integrated into the full system analysis to obtain a better understanding of the overall system performance.

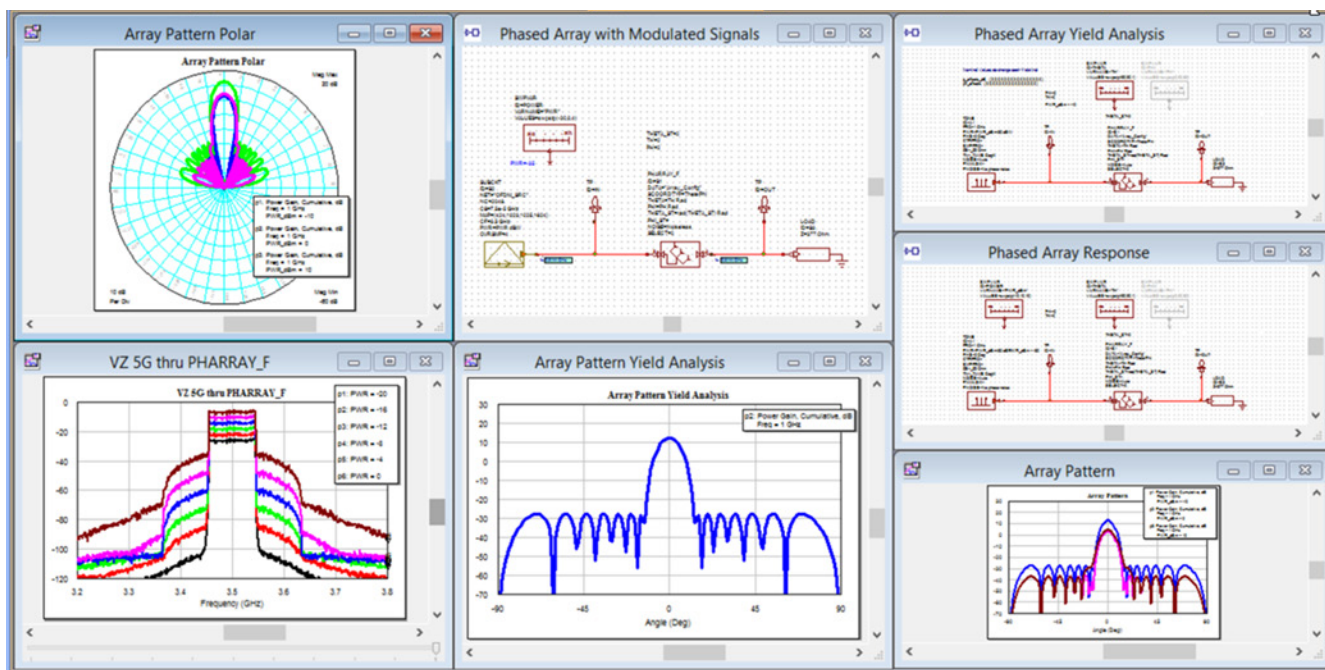


Figure 16: AWR VSS phased-array modeling captures radiated power as a function of feed power levels, RF link budget and modulated waveforms used in communication systems

## Phased-Array Antenna Features

Novel capabilities for full system analysis of actively-steered phased-array antennas are offered by AWR VSS software. The simulator provides full system performance as a function of steered beam direction, the antenna design, and active and passive circuit elements used to implement the electronic beam steering.

System analysis enables designers to:

- ▶ Evaluate array performance for over a range of power levels and/or frequencies
- ▶ Perform budget analysis measurements such as cascaded gain, NF, P1dB, and gain-to-noise temperature (G/T)
- ▶ Evaluate sensitivity to imperfections and hardware impairments via yield analysis
- ▶ Perform end-to-end system simulations using a complete model of the phased array

In addition, parametric analysis allows the designer to efficiently study changes in the system design to balance cost versus system performance. Examples of parametric studies include T/R module specifications, phase-shifter errors (number of bits), combiner/divider topologies, resistive versus reactive amplitude shaping, the number of antenna elements, and antenna element spacing.

AWR VSS software further offers phased-array simulation capability that enables modeling of phased arrays with thousands of antenna elements. It allows array configuration using various standards, as well as custom geometries. The phased array's behavior can be easily defined through the parameter dialog box or through a data file containing configuration parameters such as gain and phase offset, theta/phi angles of incidence, x/y location (length units or lambda-based, and signal frequency). The phased-array model can be set to either TX or RX modes. In TX mode, the signal power exciting each element is calculated based on the signal setting defined by the user with options that include:

- ▶ Lossless – excites all array elements by the power of the input signal
- ▶ Power divider – the input signal is divided equally among all array elements
- ▶ Voltage divider – the input signal is divided equally among all array elements such that the sum of their voltages equals the input signal

Control of the amplitude excitation through gain tapering is often used for beam shaping and to reduce the sidelobe levels. A number of commonly used gain tapers are implemented in the phased-array block. Gain taper coefficient handling defines whether the gain taper is normalized or not. If it is, the taper is normalized to unit gain. Standard gain tapers implemented in the phased-array model include Dolph-Chebyshev, Taylor Hansen, and uniform. In addition, the user can define custom gain tapers by specifying the gains (dB) and phases for each array element, as shown in Figure 17.

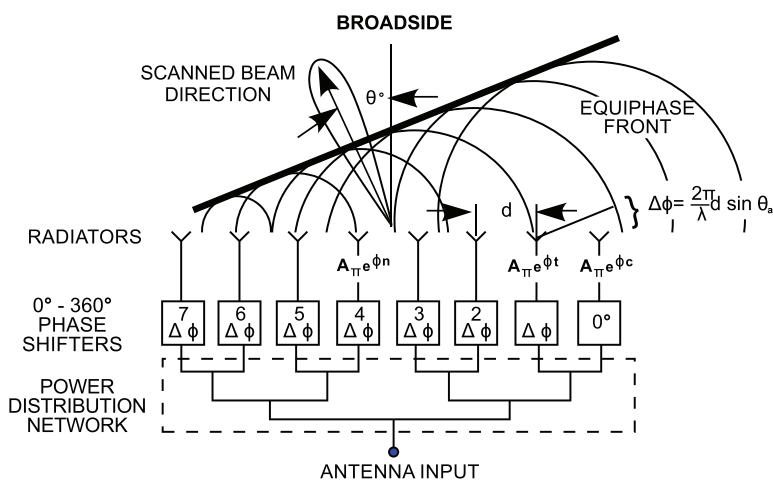


Figure 17. Gain tapering for beam shaping/steering and sidelobe control

Along with various signal distribution schemes and support for the frequency-dependent operation, the model also allows the user to simulate array imperfections due to manufacturing flaws or element failure. All gain/phase calculations are performed internally, and yield analysis can be applied to the block in order to evaluate sensitivity to variances of any of the defining phased array parameters.

The parameter dialog box enables the user to quickly define an antenna-array architecture using standard or custom geometries. The lattice option allows configuration of the phased array in a lattice pattern using the number of elements along the X and Y axes,  $n_x$  and  $n_y$ , element spacing along these axes,  $d_x$  and  $d_y$ , and  $\gamma$ , the angle between these axes. Setting  $\gamma$  to 90 degrees results in a rectangular lattice while setting it to 60 degrees creates a triangular lattice. Any positive value for  $\gamma$  may be used to configure the lattice while the circular option enables the configuration of circular phased arrays with one or more concentric circles. The number of elements in each concentric circle and the radius of each circle can be defined as vectors by variables  $n_c$  and  $r$ . Examples of lattice and circular array configurations are shown in Figure 18. Alternately, the user-defined option allows for custom array architectures, using the number of array elements,  $n$ , and their x/y locations.

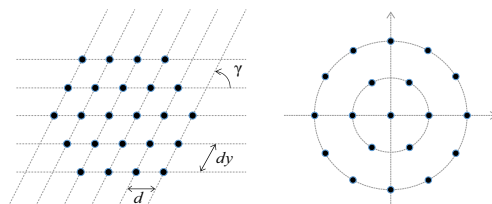


Figure 18: Standard array geometries for phased arrays in AWR VSS software (lattice and circular)

Designers can define gains or full radiation patterns for each antenna element (Figure 19) in the phased array. This enables them to use different radiation patterns for internal, edge, and corner elements of the phased array. The radiation pattern of each antenna element will often be affected by its position in the phase array. These patterns can be measured in the lab or calculated in the integrated AXIEM planar 3D and Analyst 3D FEM EM simulators. A simple approach is to use a 3x3 phased array and excite one element—either the internal element, one of the edge elements, or one of the corner elements—while terminating all others. This will provide the internal, edge, and corner element radiation patterns, which can then be automatically stored in data sets using AWR Design Environment output data measurements. This approach includes the effect of mutual coupling from first-order neighbors. A 5x5 element array may also be used to extend mutual coupling to first- and second-order neighbors.

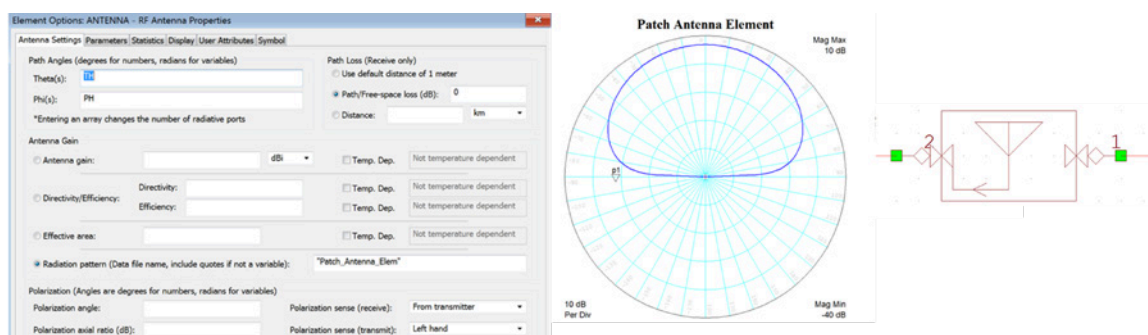


Figure 19: Single-element patch antenna

## RF Link Modeling

AWR VSS software also boasts the capability to model the RF links of individual elements in the phased array. This is an important function since RF links are not ideal and can cause the array behavior to deviate significantly from its ideal one. As an example, gain tapers are commonly used in phased arrays; however, when identical RF links are used for all antenna elements, this may cause certain elements (the ones with higher gains) to operate near or in compression while others in a pure linear region. In this case, the array performance will be significantly impacted by how close to compression the elements are operating. Alternatively, based on the gain tapers that are used, designers may choose to use different RF link designs for different elements. While this is a more complicated task, it will result in more efficient phased arrays. AWR VSS phased-array modeling allows designers to achieve uniform RF link design to all elements or at least account for the performance degradation from uneven RF links to each element. Being able to predict such performance and modify the RF designs so that requirements are met is one of the unique capabilities that the AWR VSS phased-array modeling functionality offers.

As AESA radar systems become more sophisticated with increased element counts and antenna/electronics integration advances, the capability to design and verify the performance of the individual components along with the entire signal channel is becoming critical. AWR software provides circuit simulation, system-level behavioral modeling, and EM analysis operating within a single platform enabling development teams to investigate system performance and component-to-component interaction prior to costly prototyping.

## MIMO/Phased-Array Antenna Systems

Phased-array antennas are becoming popular for a variety of applications such as automotive driver assist systems, satellite communications, advanced radar, and more. The complexity and cost issues involved in developing communications systems based on phased-array antennas are being addressed through new functionalities in EDA software that support designers with the means to develop new system architectures and component specifications, as well as implement the physical design of individual components and verify performance prior to prototyping. This application note discusses these trends and presents recent advances in EDA tools for phased-array-based systems.

### Design Management and EDA Tools

While actively-steered phased-array antennas have many advantages, they are extremely complex, and their production, especially non-recurring development costs, is significantly higher than for conventional antenna design. As the industry shifts toward highly-integrated phased-array systems, it is critical for in-house systems expertise to work closely with hardware developers, with both fully exploring the capabilities and tradeoffs among possible architectures and integration technologies. In addition, a start-to-finish design flow made possible with EDA software has become critical in moving beyond the initial system simulation, which is focused on early architecture definition, to the development of link budgets and component specifications.

A preferred phased-array system design flow manages the start-to-finish front-end development, embedding RF/microwave circuit simulation and/or measured data of radio/signal-processing (behavioral) models within a phased-array system hierarchy. Such software enables the system designer to select the optimum solution, ranging from hybrid modules through fully-integrated silicon core RF integrated circuit (IC) devices, addressing the specific requirements of the targeted application. Perhaps more importantly, a system-aware approach, carried throughout the entire phased-array development cycle, enables the team to continually incorporate more detail into their predictive models, observe the interactions between array components, and make system adjustments as the overall performance inadvertently drifts from early idealized simulations.

Design failure and the resulting high costs of development are often due in part to the inability of high-level system tools to accurately model the interactions between the large number of interconnected channels, which are typically specified and characterized individually. Since overall phased-array performance is neither driven purely by the antenna nor by the microwave electronics in the feed network, simulation must capture their combined interaction in order to accurately predict true system behavior. Circuit, system, and EM co-simulation enables verification throughout the design process.

### Phased-Array Design Flow

A leading phased-array design flow is available with AWR VSS software, which provides full system performance as a function of steered-beam direction, inclusive of the antenna design, and the active and passive circuit elements used to implement the electronic beam steering. System components can be modeled in greater detail using AWR Microwave Office® circuit simulation, inclusive of EM analysis for antenna design and passive device modeling using AWR AXIEM® 3D planar and Analyst™ 3D FEM EM simulators.

These tools are fully integrated into AWR Design Environment software, supporting seamless data sharing within the phased-array hierarchy. Furthermore, individual antenna designs can be generated from performance specifications using the AntSyn antenna synthesis and optimization module, with resulting geometries imported into AXIEM or Analyst software for further EM analysis and optimization.

Highlights of phased-array analysis in AWR VSS software include:

- ▶ Automate/manage the implementation of beamforming algorithms and determine phased-array antenna configuration from a single input/output block
- ▶ Accomplish array performance for over a range of user-specified parameters such as power level and/or frequency.
- ▶ Perform various link-budget analyses of the RF feed network, including measurements such as cascaded gain, noise figure (NF), output power (P1dB), gain-to-noise temperature (G/T), and more
- ▶ Evaluate sensitivity to imperfections and hardware impairments via yield analysis
- ▶ Perform end-to-end system simulations using a complete model of the phased array
- ▶ Simulate changing array impedance as a function of beam angle to study the impact of impedance mismatch and gain compression on front-end amplifier performance

## Defining Phased-Array Configurations

Specifications for any phased-array radar are driven by the platform requirements and the intended application. For example, weather observation, which has relied on radar since the earliest days of this technology, most commonly uses airborne surveillance radar to detect and provide timely warnings of severe storms with hazardous winds and damaging hail. The weather surveillance radars are allocated to the S (~ 10cm wavelength), C (~ 5cm wavelength), and X (~ 3cm wavelength) frequency bands. While the shorter wavelength radars provide the benefit of a smaller antenna size, their radiated signals are significantly affected by atmospheric attenuation.

Requirements for 10cm wavelength (S-band) weather surveillance radars, based on years of experience with the national network of non-Doppler radars (WSR-57), are shown in Figure 20.<sup>1</sup>

1.1.1 Range:	460 km
1.1.2 Time:	< 5 minutes
1.1.3 Volumetric coverage:	hemispherical
1.2. SNR:	> 10 dB, for Z . 15 dBZ at r = 230 km
1.3. Angular resolution:	≤1°
1.4. Range sample interval $\Delta r$	
1.4.1 for reflectivity estimates:	$\Delta r < 1 \text{ km}; 0 < r < 230 \text{ km}$
1.4.2 for velocity and spectrum width estimates ( $r < 230 \text{ km}$ ):	$\Delta r < 2 \text{ km}; r < 460 \text{ km}$
1.5. Estimate accuracy:	
1.5.1 reflectivity:	≤1 dB
1.5.2 velocity:	≤1 m s <sup>-1</sup> ; SNR> 8 dB; $\sigma_v = 4 \text{ m s}^{-1}$
1.5.3 spectrum width:	≤1 m s <sup>-1</sup> ; SNR>10 dB; $\sigma_v = 4 \text{ m s}^{-1}$

Figure 20: Requirements for 10cm wavelength weather surveillance radars

These requirements showcase some of the application-specific metrics that drive range, frequency, antenna size, and gain. These factors represent the starting point for the system designer, who will also weigh the cost and delivery concerns and available semiconductor and integration technologies when considering possible architectures and defining individual component performance targets.

AWR VSS software provides system designers with the capabilities needed to convert these requirements into hardware specifications and work out the initial design details. Starting with the phased-array configuration, AWR VSS software is able to represent thousands of antenna elements with a single model, enabling the antenna design team to quickly produce radiation patterns with basic array properties such as number of elements, element spacing, individual element gain, or radiation pattern (imported measured or simulated antenna data), array configuration, and gain taper. The model, shown in Figure 21, allows designers to specify the array’s physical configuration based on various standard lattice and circular geometries, as well as custom geometries.

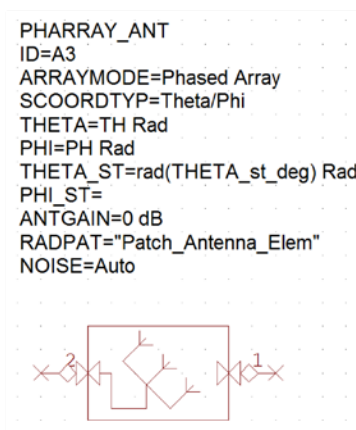


Figure 21: Single phased-array elements can model large scale (thousands of elements) arrays

1. [https://www.nssl.noaa.gov/publications/mpar\\_reports/LMCO\\_Consult2.pdf](https://www.nssl.noaa.gov/publications/mpar_reports/LMCO_Consult2.pdf)

The array behavior is easily defined through a parameter dialog box or a data file containing configuration parameters such as gain and phase offset, theta/phi angles of incidence, number of elements in both X/Y locations (length units or lambda-based), spacing, and signal frequency. This model greatly simplifies early exploration of large-scale phased array configurations and individual antenna performance requirements versus the old method of implementing such a model using basic individual blocks, where array sizes were generally limited to several hundred elements, each modeled as a single input/single output block.

Figure 22 shows a portion of the AWR VSS parameter dialog box used to quickly define an antenna-array architecture using standard or custom geometries. The lattice option allows configuration of the phased array in a lattice pattern, which is configured using the number of elements along the X and Y axes, NX and NY, element spacing along these axes, dx and dy, and gamma, the angle between these axes. Setting gamma to 90° results in a rectangular lattice, while setting it to 60° creates a triangular lattice. Any positive value for gamma may be used to configure the lattice, while the circular option enables the configuration of circular phased arrays with one or more concentric circles. The number of elements in each concentric circle and the radius of each circle can be defined as vectors by variables NC and R. Examples of lattice and circular array configurations are shown in Figures 23.

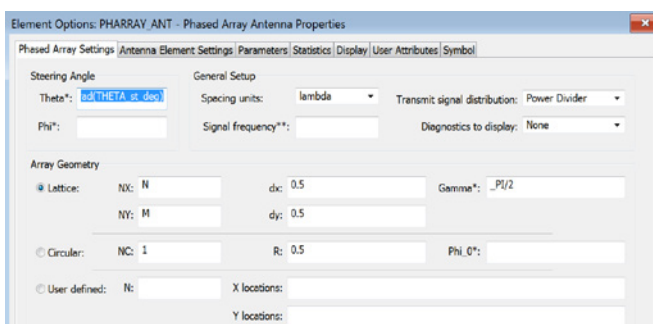


Figure 22: Phased-array parameter dialog box

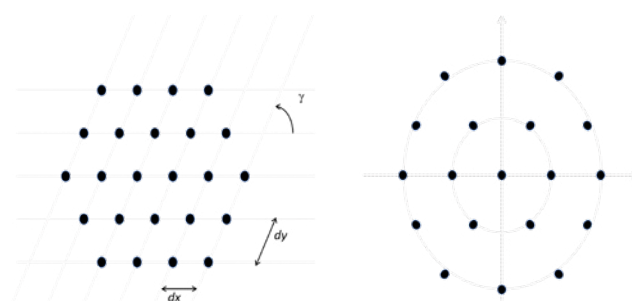


Figure 23. Standard AWR VSS array geometries: lattice (left), circular (right)

To demonstrate some of the capabilities of the phased-array model, an example project was constructed showing two 15x5 element arrays operating at 2.99GHz (Figure 24).

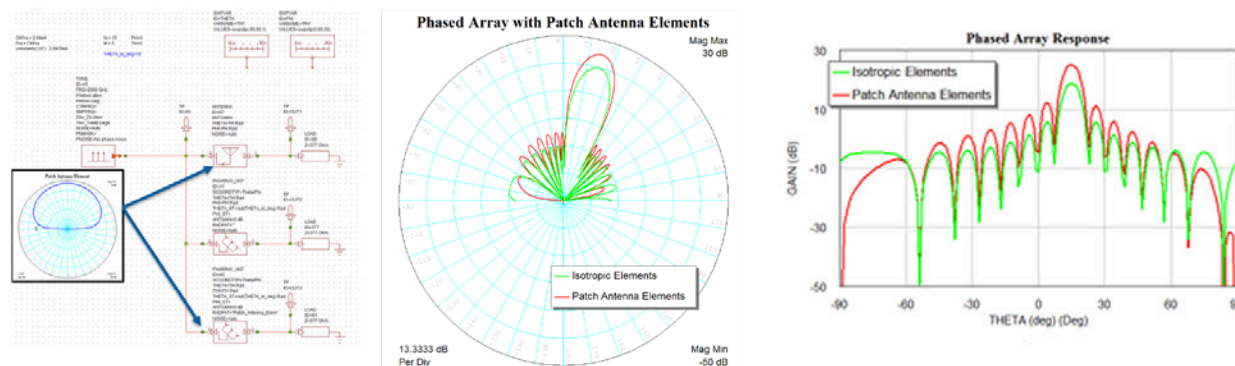


Figure 24. Two 15x5 element phased arrays based on isotropic and patch antenna radiation patterns with theta angle set to 15°

One model represents an array of lossless isotropic antennas defined simply by setting the antenna gain to 0 dBi, while the elements of the other array utilize a data set containing the radiation pattern of a single simulated patch antenna. Both arrays use a lattice configuration with a  $1/2\lambda$  spacing between elements and uniform gain tapering - explained in more detail below. For the simulation shown, the steering angle (theta) was set to  $15^\circ$ . Note that the antenna and phased-array blocks support specifying the signal direction using U/V coordinates as well as theta/phi angles (Figure 25).

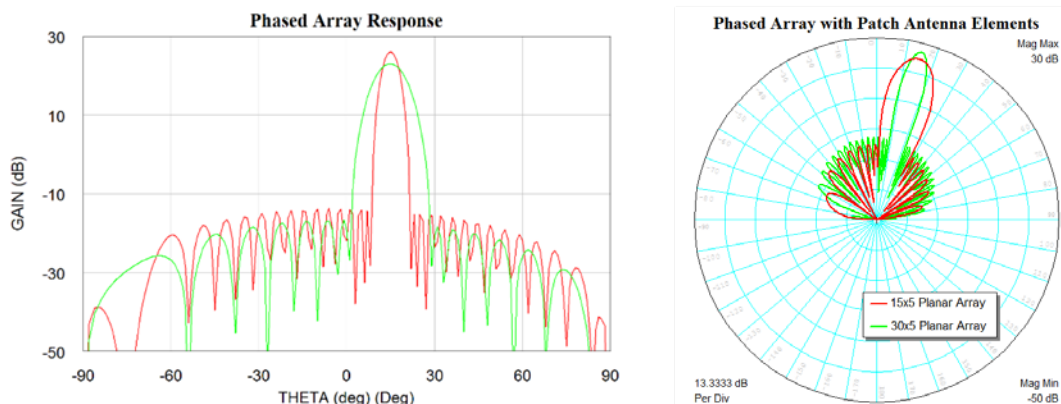


Figure 25: Radiation patterns for 15x5 and 30x5 arrays and sidelobe behavior for array (5x15)

The AWR VSS array model provides antenna designers with a rapid and straightforward tool to observe key antenna metrics, providing a means to examine the main beam and sidelobe behavior as a function of any number of variables, including array size and configuration, gain versus steering angle, and the occurrence of grating lobes as a function of element spacing and/or frequency. From these results, the array design team can develop an optimum configuration for the given requirements such as range and overall array physical size. In addition, the team can provide design targets for the individual antennas and incorporate subsequent antenna simulation results back into the array analysis.

Control of the amplitude excitation through gain tapering is often used to control beam shape and reduce the sidelobe levels. A number of commonly-used gain tapers are implemented in the phased-array block. Gain taper coefficient handling defines whether the gain taper is normalized or not. If it is, the taper is normalized to unit gain. Standard gain tapers implemented in the phased-array model include Dolph-Chebyshev, Taylor Hansen, and uniform. The earlier example (15x5 element patch array) was re-simulated with uniform versus Dolph-Chebyshev gain tapering, showing the impact on the main beam and sidelobes, as shown in Figure 26. In addition, the user can define custom gain tapers by specifying the gains (dB) and phases for each array element.

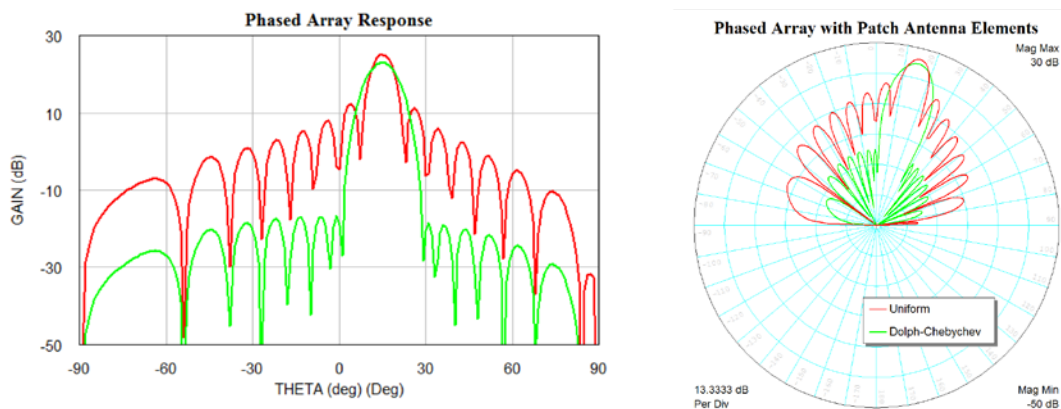


Figure 26: 5x15 patch array with uniform vs. Dolph-Chebyshev gain tapering



This simulation provided the antenna pattern used to replace the original patch antenna used in the 15x5 phased array, with the new antenna pattern shown in Figure 29. The new phased-array results for both the original antenna (red trace) and the square-ring patch (green trace) are shown in Figure 29 as well.

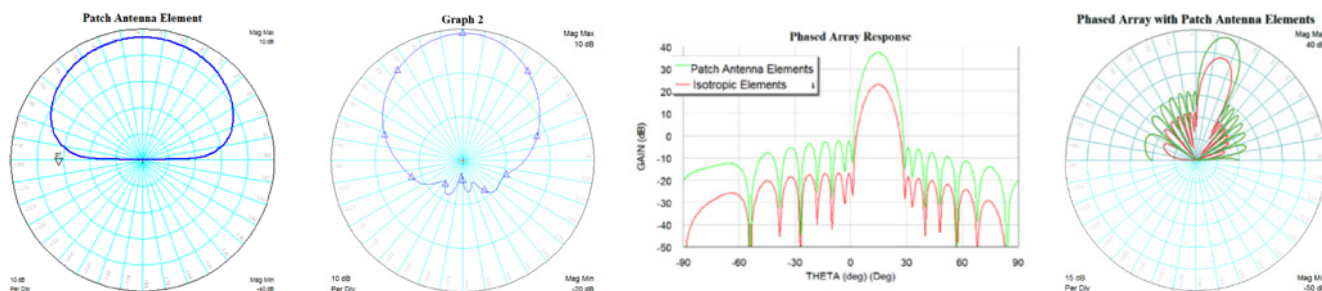


Figure 29: Patterns of single-patch and square-ring antennas generated by AntSyn and comparison of radiation patterns from phased arrays based on simple patch antenna (red) and square-ring patch antenna (green)

### Modeling Complex Interactions

The mutual coupling between antenna elements affects antenna parameters like terminal impedances and reflection coefficients, and hence the antenna-array performance in terms of radiation characteristics, output signal-to-interference noise ratio (SINR), and RCS. AWR VSS software includes capabilities for more accurate simulation of these parameters, including enhanced modeling of element patterns and mutual coupling. The next section of this article will examine these recent advances in advanced phased-array modeling, including an accurate representation of the feed structure.

As mentioned, in AWR VSS designers can define gains or full radiation patterns for each antenna element in the phased array. This enables them to use different radiation patterns for internal, edge, and corner elements of the phased array (Figure 30).

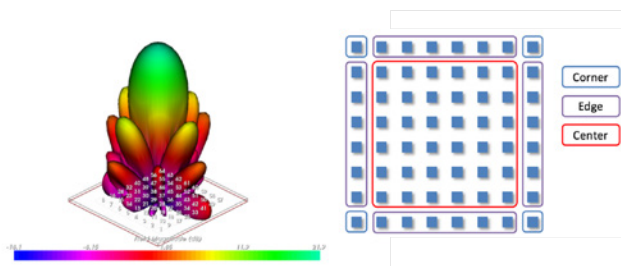


Figure 30: Supports the ability to assign different antenna patterns to individual elements

The radiation pattern of each antenna element will likely be affected by its position in the phased array. These patterns may be measured in the lab or calculated in AXIEM or Analyst software. A simple approach to characterizing the appropriate radiation pattern for a given element is to use a 3x3 phased array and excite one element, either the internal element, one of the edge elements, or one of the corner elements while terminating all others. This will provide the internal, edge, and corner element radiation patterns, which can then be automatically stored in data files using the AWR software output data file measurements (the same technique used in the example above). This approach includes the effect of mutual coupling from first-order neighbors. An array with a larger number of elements may be used to extend mutual coupling to first- and second-order neighbors.

It is also important to capture the mutual coupling between neighboring elements. The AWR VSS phased-array model does this through a coupling table defined in the configuration file. Different coupling levels can be defined based on distance from each other. The coupling, which is specified in magnitude (dB) and phase (degrees), is defined for two different distances (adjacent side elements: radius c\_1 and adjacent corner elements: radius c\_2) (Figure 31).

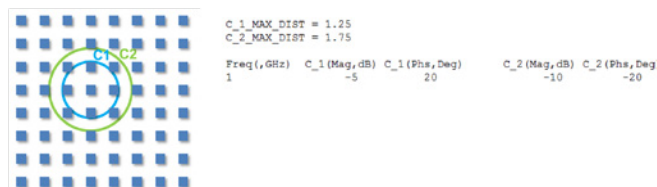


Figure 31: 64-element array showing mutual coupling table

## Modeling Impairments and Yield Analysis

RF hardware impairments of the array will affect the resulting sidelobe levels and beam patterns and will ultimately reduce system-level performance. For transmitter arrays, sidelobe levels from imperfectly formed beams may interfere with external devices or make the transmitter visible to countermeasures. In radar systems, sidelobes may also cause a form of self-induced multipath, where multiple copies of the same radar signal arrive from different sidelobe directions, which can exaggerate ground clutter and require expensive signal processing to remove. Therefore, it is critical to identify the source of such impairments, observe their impact on the array performance, and take steps to reduce or eliminate them.

The AWR VSS phased-array configuration file allows engineers to simulate array imperfections due to manufacturing flaws or element failure. All gain/phase calculations are performed internally, and yield analysis can be applied to the block in order to evaluate sensitivity to variances of any of the defining phased-array parameters. As an example, AWR VSS software was used to perform an element failure analysis on a 64-element (v array, producing the plots in Figure 32, which illustrates the sidelobe response degradation.

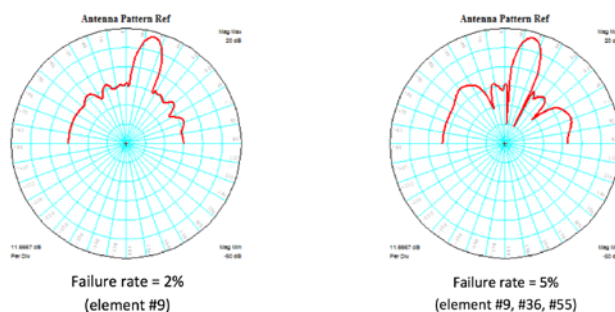


Figure 32: Sidelobe degradation to element failures 2% and 5%

RF impairments can also be caused by any number of items relating to the feed network design and related components. Systematic errors that may be compensated include inter-chain variations caused by asymmetrical routing (layout), frequency dependencies, noise, temperature, and varied mismatching due to changing antenna impedance with steer angle, which also impacts amplifier compression. Therefore, it is imperative to be able to simulate the interactions between the antenna array and the individual RF links in the feed network.

## RF Link Modeling

AWR software products include the simulation and modeling technology to capture these impairments accurately and incorporate these results into the AWR VSS phased-array assembly model. This is an important functional since RF links are not ideal and can cause the array behavior to deviate significantly. The phased-array assembly can operate in either the RX or TX mode, supporting the configuration of the array-element geometry, each element's antenna characteristics, the RF link characteristics, and the common linear characteristics of the combiner/splitter used to join the elements together. The configuration is performed primarily through a text data file, with commonly-swept settings either specified directly via block parameters (such as steering angles) or specified in the data file but capable of being overridden via block parameters (such as individual element gain and phase adjustments).

The configuration of the phased-array assembly can be divided into several sections:

- ▶ Array geometry - defines the number of elements, their placement, and any geometry-related gain and phase tapers
- ▶ Antenna characteristics - defines antenna gain, internal loss, polarization loss, mismatch loss, and radiation patterns for both receive and transmit configurations
- ▶ RF link characteristics - defines links for individual elements including gain, noise, and P1dB. Supports 2-port RF nonlinear amplifiers using large-signal nonlinear characterization data typically consisting of rows of input power or voltage levels and corresponding output fundamental, harmonic, and/or intermodulation product levels. Frequency-dependent data is also supported
- ▶ Assignment of antenna and RF link characteristics to individual elements.
- ▶ Power splitter characteristics - splits the incoming signal into n-connected output ports
- ▶ Mutual coupling characteristics (previously discussed)

One common challenge is that not all RF links should be equal. For example, gain tapers are commonly used in phased arrays; however, when identical RF links are used for all antenna elements, elements with higher gains may operate well into compression while others operate in a purely linear region, causing undesired array performance. To avoid this problem, designers often use different RF link designs for different elements. While this is a more complicated task, AWR VSS phased-array modeling enables them to achieve this, resulting in more efficient phased arrays.

To assist the design team in creating the feed network and providing the RF link to the systems team, AWR VSS software includes the capability to automatically generate the characteristics of the phased-array element link defined by the data tables. The designer starts by creating a schematic-based link design per the system requirements. A “measurement” extracts the design characteristics, which can include circuit-level design details (nonlinearities), through Microwave Office co-simulation and saves a properly-formatted data file for use with the phased-array assembly model.

### In-Situ Nonlinear Simulations

An accurate simulation must also account for the interactions that occur between the antenna elements and the driving feed network. The problem with simulation software is that the antenna and the driving feed network influence each other. The antenna’s pattern is changed by setting the input power and relative phasing at its various ports. At the same time, the input impedances at the ports change with the antenna pattern. Since input impedance affects the performance of the nonlinear driving circuit, the changing antenna pattern affects overall system performance.

In this case, the input impedance of each element in the array must be characterized for all beam-steering positions. The array is only simulated once in the EM simulator. The resulting S-parameters are then used by the circuit simulator, which also includes the feed network and amplifiers. As the phase shifters are tuned over their values, the antenna’s beam is steered. At the same time, each amplifier sees the changing impedance at the antenna input to which it is attached, which affects the amplifier’s performance.

In this final example, the power amplifiers (PAs) are nonlinear, designed to operate at their 1-dB compression point (P1dB) for maximum efficiency. They are, therefore, sensitive to the changing load impedances presented by the array. The beam of a 16-element array is steered by controlling the relative phasing and attenuation to the various transmit modules (Figure 33). In practice, the harmonic balance simulation in Microwave Office software used to characterize the power amplifiers takes substantial time to run with 16 PAs. Therefore, the beam is steered with the amplifiers turned off. The designer then turns on the individual PA for specific points of interest once the load impedance from the directed antenna has been obtained.

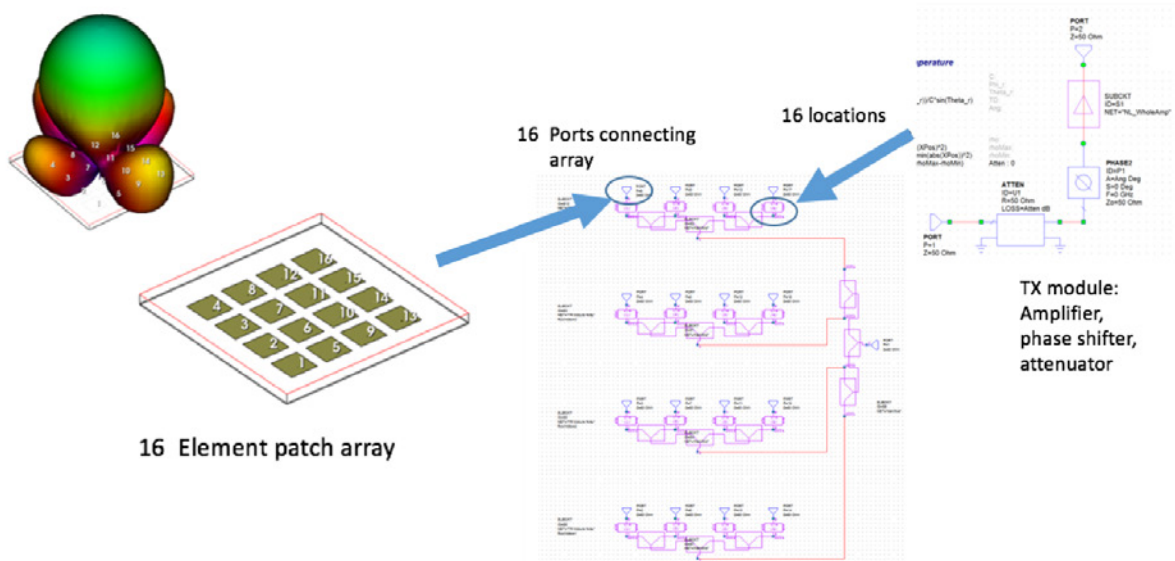


Figure 33: Changing antenna feed impedance as a function of beam steering using the variable phase and attenuator settings defined in the feed network design

At this point, the designer can directly investigate the PA nonlinear behavior as a function of the load (antenna) impedance. With the load-pull capability in Microwave Office software, PA designers can investigate output power, compression, and any other number of nonlinear metrics defining the amplifier’s behavior, as shown in Figure 34.

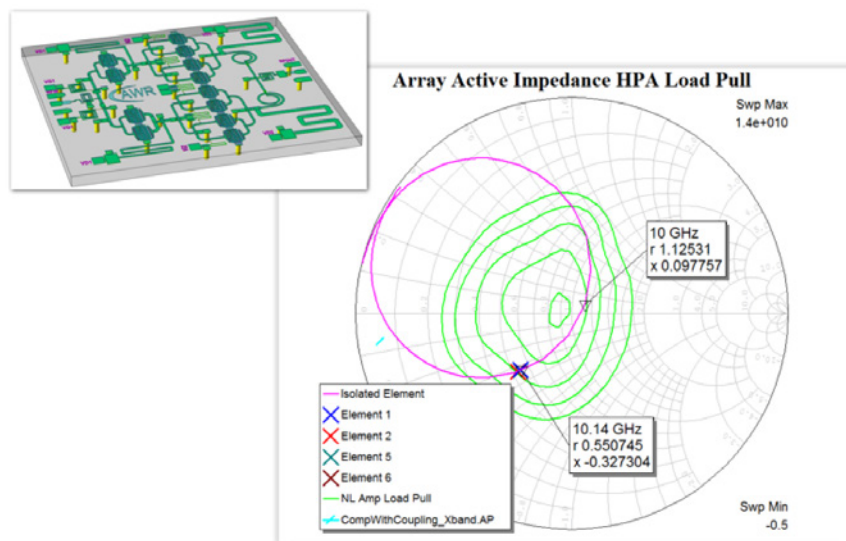
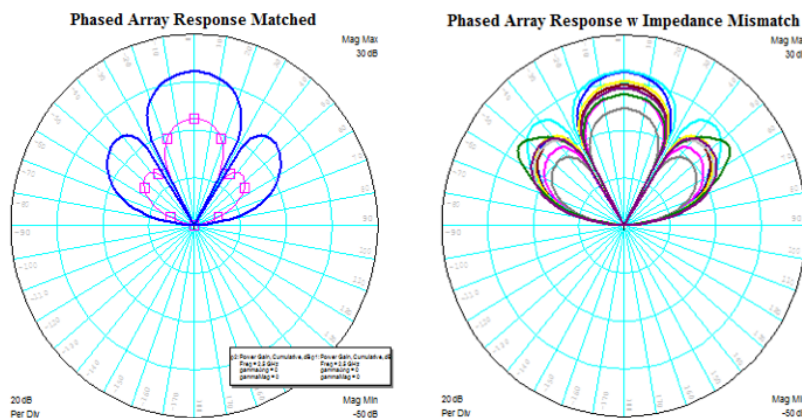


Figure 34: Simulated antenna feed impedance vs. frequency, superimposed over power load-pull contours for a broadband MMIC PA (inset)

With a detailed characterization of the RF links for each element, the overall system simulation is able to indicate trouble areas that would have previously gone undetected until expensive prototypes were made and tested in the lab (Figure 35).

Figure 35: Phased-array simulations with RF link effects, including the impact of impedance mismatch between PA and steered antenna array



The capability to design and verify the performance of the individual components, along with the entire signal channel that defines the AESA radar, is a necessity as element counts increase and antenna /electronics integration advances. Through a sophisticated design flow that encompasses circuit simulation, system-level behavioral modeling, and EM analysis operating within a single design platform, development teams can investigate system performance and component-to-component interaction prior to costly prototyping.

## mmWave Automotive Radar and Antenna System Development

As modern vehicle development expands to include more and more sophisticated electronics, automobile manufacturers are equipping their new models with advanced driver-assistance systems (ADAS) to obtain high safety ratings by increasing automotive safety. Most road accidents occur due to human error, and ADAS are proven to reduce injuries and fatalities by alerting drivers to and assisting them with a variety of issues, including collision avoidance and low tire pressure using radar technology mostly focused over the 76 to 81GHz spectrum. They perform over a range of applications, operating conditions, and object detection challenges in order to provide reliable coverage over the range (distance) and field of view (angle) as dictated by the particular driver-assist function.

This application example presents some of the challenges behind developing millimeter-wave (mmWave) radar systems and the antenna array technologies for the next generation of smart cars and trucks. Examples will be presented demonstrating how the AWR Design Environment platform, specifically the radar design capabilities within AWR VSS system design software, can be used successfully in ADAS applications.

### ADAS Technology

ADAS is made possible through a network of sensors that perform specific safety functions. Manufacturers are currently implementing these systems based on vision sensor technology and radar systems operating at either 24 and/or 77GHz. Vision systems detect lane markings and process other visual road information, however, they are susceptible to inadequate performance due to precipitation, particularly snow and fog, as well as distance.

On the other hand, long-range radar (LRR) supports multiple functions, comfortably handling distances between 30 and 200 meters, and short-range radar (SRR) can detect objects below 30-meter distances. While the 24GHz frequency band, which addresses SRR detection, is expected to be phased out of new vehicles by 2022, today it is commonly found in hybrid architectures. Meanwhile, the 77GHz band (from 76–81GHz) supporting LRR is expected to provide both short and long-range detection for all future automotive radars. Figure 36 provides details on short/medium and long-range radar.

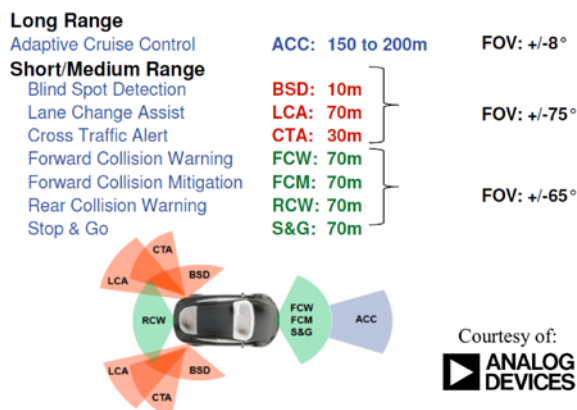


Figure 36: Different ranges, fields of view (FOV), and functions for advanced driver assist systems

Technical advantages of the 77GHz band include smaller antennas (a third of the size of the current 24GHz ones), higher permitted transmit power, and, most importantly, wider available bandwidth, which enables higher object resolution. As a result, advances in radar modulation techniques, antenna beam steering, system architecture, and semiconductor technology are driving the rapid adoption of mmWave radar in future ADAS enabled cars and trucks.

To manage the adoption of these technologies, radar developers require RF-aware system design software that supports radar simulations with detailed analysis of RF front-end components, including nonlinear RF chains, advanced antenna design, and channel modeling. Co-simulation with circuit and EM analysis provides an accurate representation of true system performance prior to building and testing costly radar prototypes. AWR software provides these capabilities, all within a platform that manages automotive radar product development— from initial architecture and modulation studies through the physical design of the antenna array and front-end electronics based on either III-V or silicon integrated circuit (IC) technologies.

The AWR Design Environment platform integrates these critical radar simulation technologies while providing the necessary automation to assist the engineering team with the very complex task of managing the physical and electrical design data associated with ADAS electronics. ADAS support includes:

- ▶ Design of waveforms, baseband signal processing, and parameter estimation for radar systems, with specific analyses for radar measurements along with comprehensive behavioral models for RF components and signal processing.
- ▶ Design of transceiver RF/microwave front-end with circuit-level analyses and modeling (distributed transmission lines and active and passive devices) to address printed circuit board (PCB) and MMIC/RFIC design.
- ▶ Planar/3D EM analysis for characterizing the electrical behavior of passive structures, complex interconnects, and housings, as well as antennas and antenna arrays.
- ▶ Connection between simulation software and test and measurement instruments.

### Radar Architectures and Modulation

For adaptive cruise control (ACC), simultaneous target range and velocity measurements require both high resolution and accuracy to manage multi-target scenarios such as highway traffic. Future developments targeting safety applications like collision avoidance (CA) or autonomous driving (AD) call for even greater reliability (extreme low false alarm rate) and significantly faster reaction times compared to current ACC systems, which utilize relatively well-known waveforms with long measurement times (50–100 ms).

Important requirements for automotive radar systems include the maximum range of approximately 200m for ACC, a range resolution of about 1m, and a velocity resolution of 2.5 km/h. To meet all these system requirements, various waveform modulation techniques and architectures have been implemented, including a CW transmit signal or a classical pulsed waveform with ultra-short pulse length.

The main advantages of CW radar systems in comparison with pulsed waveforms are the relatively low measurement time and computation complexity for a fixed high-range resolution system requirement. The two classes of CW waveforms widely reported in the literature include linear-frequency modulation (LFMCW) and frequency-shift keying (FSK), which use at least two different discrete transmit frequencies. Table 1 compares the different radar architectures and their advantages and disadvantages.

	Pulse Doppler	FMCW	FSK	UWB
Signals/Plots				
Description	<ul style="list-style-type: none"> <li>▶ Single-carrier frequency is transmitted in a short burst</li> </ul>	<ul style="list-style-type: none"> <li>▶ Typically a sawtooth waveform with 100 - 150MHz bandwidth</li> </ul>	<ul style="list-style-type: none"> <li>▶ FSK with 1MHz steps</li> <li>▶ Coherent processing interval (CPI) per frequency is 5 ms</li> <li>▶ Range info is derived from phase difference</li> </ul>	<ul style="list-style-type: none"> <li>▶ Dirac pulse</li> <li>▶ Measure time-of-flight auto correlation</li> </ul>
Advantages	<ul style="list-style-type: none"> <li>▶ Simple algorithm for distance</li> </ul>	<ul style="list-style-type: none"> <li>▶ Good range accuracy</li> <li>▶ Easy to calculate relative speed and range</li> </ul>	<ul style="list-style-type: none"> <li>▶ Simple voltage controlled oscillator (VCO) modulation</li> <li>▶ Short measurement cycle</li> </ul>	<ul style="list-style-type: none"> <li>▶ Simple principle</li> <li>▶ Can measure at close range due to large BW</li> </ul>
Disadvantages	<ul style="list-style-type: none"> <li>▶ Difficult-to-determine range rate</li> <li>▶ Cannot transmit and receive simultaneously</li> </ul>	<ul style="list-style-type: none"> <li>▶ Computation to eliminate ghost targets</li> <li>▶ Long measurement time for multiple chirps</li> </ul>	<ul style="list-style-type: none"> <li>▶ Coherent signal required for accuracy</li> <li>▶ Poor range direction information</li> </ul>	<ul style="list-style-type: none"> <li>▶ Medium-to-low range</li> <li>▶ No direct measure of range rate</li> <li>▶ Sensitive to disturbance</li> </ul>

Table 1: Different radar architectures and their technical advantages/disadvantages in target detection, range, robustness, and resolution

For ACC applications, simultaneous range and relative velocity are of utmost importance. While LFM CW and FSK fulfill these requirements, LFM CW needs multiple measurement cycles and mathematical solution algorithms to solve ambiguities, while FSK lacks in range resolution. As a result, a technique combining LFM CW and FSK into a single waveform called multiple frequency shift keying (MFSK) is of considerable interest. MFSK was specifically developed to serve radar development for automotive applications and consists of two or more transmit frequencies with an intertwined frequency shift and with a certain bandwidth and duration, as shown in Figure 37.<sup>1</sup>

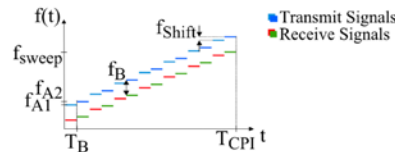


Figure 37: Multiple frequency shift keying

As previously mentioned, pulsed radars are also widely used in automotive radar systems. Relative velocity can be determined from consecutive pulses using a coherent transmitter and receiver to measure pulse-to-pulse phase variations containing the Doppler frequency that conveys relative velocity. For a pulsed-Doppler (PD) radar, the range is still measured by signal propagation time. To measure both range and relative velocity, the pulse-repetition frequency is an important parameter. There are many tradeoffs to be considered when deciding which architecture and waveform modulation technology deliver the necessary performance while maintaining development and production cost goals. These requirements can be met with AWR VSS system design software, which is dedicated to RF system design and implementation, offering a toolbox of commonly called-for simulation technologies and radio block/signal processing models, along with support for user-developed coding.

AWR VSS software is an RF and wireless communications and radar systems design solution that provides the simulation and detailed modeling of RF and digital signal processing (DSP) components necessary to accurately represent the signal generation, transmission, antenna, T/R switching, clutter, noise, jamming, receiving, signal processing, and channel model design challenges and analysis requirements for today's advanced radar systems.

The AWR VSS workspace example in Figure 38 demonstrates a possible ACC radar architecture, modulation scheme, channel modeling, and measurement configuration. This workspace includes a pulse-Doppler (PD) radar system design with signal generator, RF transmitter, antenna, clutter, RF receiver, moving target detection (MTD), constant false alarm rate (CFAR) processor, and signal detector for simulation purposes. The chirp signal level is set to 0 dBm, PRF = 2kHz and DUTY = 25%. The target model is defined by the Doppler frequency offset and target distance, and angles of arrival (THETA/PHI) are specified in a data file and vary over time. The Doppler frequency and channel delay were generated to describe the target return signal with different velocities and distances, while the radar clutter model can be included, and the power spectrum can be shaped. In this example, the clutter magnitude distribution was set to Rayleigh and the clutter power spectrum was formed by a Weibull probability distribution.

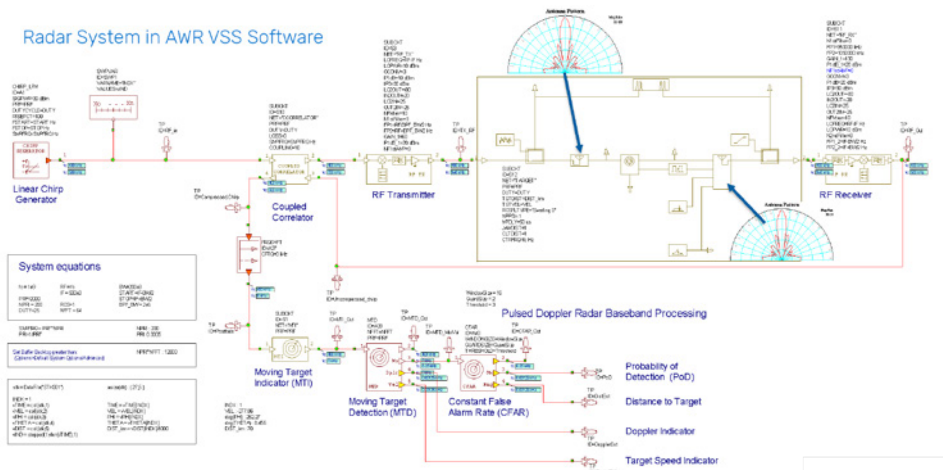


Figure 38: PD radar example

1. Rohling, Hermann; Meinecke, Marc-Michael, "Waveform Design Principles for Automotive Radar Systems," Technical University of Hamburg-Harburg, Harburg, Germany, Proceedings, 2001 CIE International Conference on Radar.

The RF transmitter in Figure 39 includes oscillators, mixers, amplifiers, and filters, whereas the gain, bandwidth, and carrier frequency were specified based on the requirements of the system or actual hardware performance as provided by the RF design team. Likewise, the RF receiver includes oscillators, mixers, amplifiers, and filters with gain, bandwidth and carrier frequency specified according to the system requirements. Co-simulation with the Microwave Office circuit simulator is possible as the transceiver front-end design details become available. As will be discussed later, the interaction between the transceiver electronics and a beamforming antenna array can be analyzed via a circuit, system, and EM co-simulation.

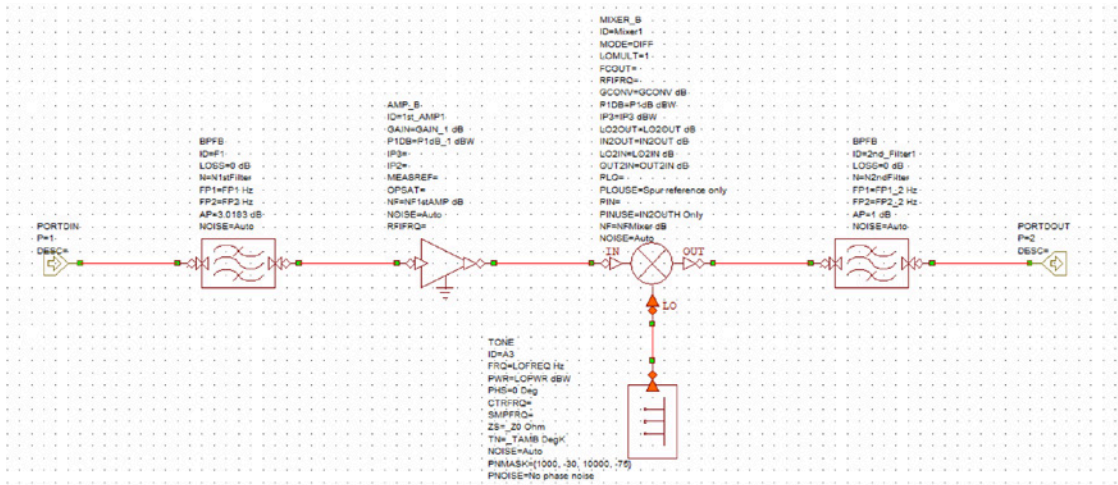


Figure 39: RF transmitter block

To detect the moving object more effectively, MTD is used. The MTD is based on a high-performance signal processing algorithm for PD radar. A bank of Doppler filters or FFT operators cover all possible expected target Doppler shifts and the output of the MTD is used for the CFAR processing. In this particular example, measurements for detection rate and CFAR are provided.

The radar signal waveform must be measured in the time domain at the receiver input. Since the target return signal is often blocked by clutter, jamming, and noise, detection in the time domain is not possible and an MTD is used to perform the Doppler and range detection in the frequency domain. In the MTD model, the data is grouped for the corresponding target range and Doppler frequency. Afterward, a CFAR processor is used to set the decision threshold based on the required probabilities of detection and false alarm, as shown in Figure 40.

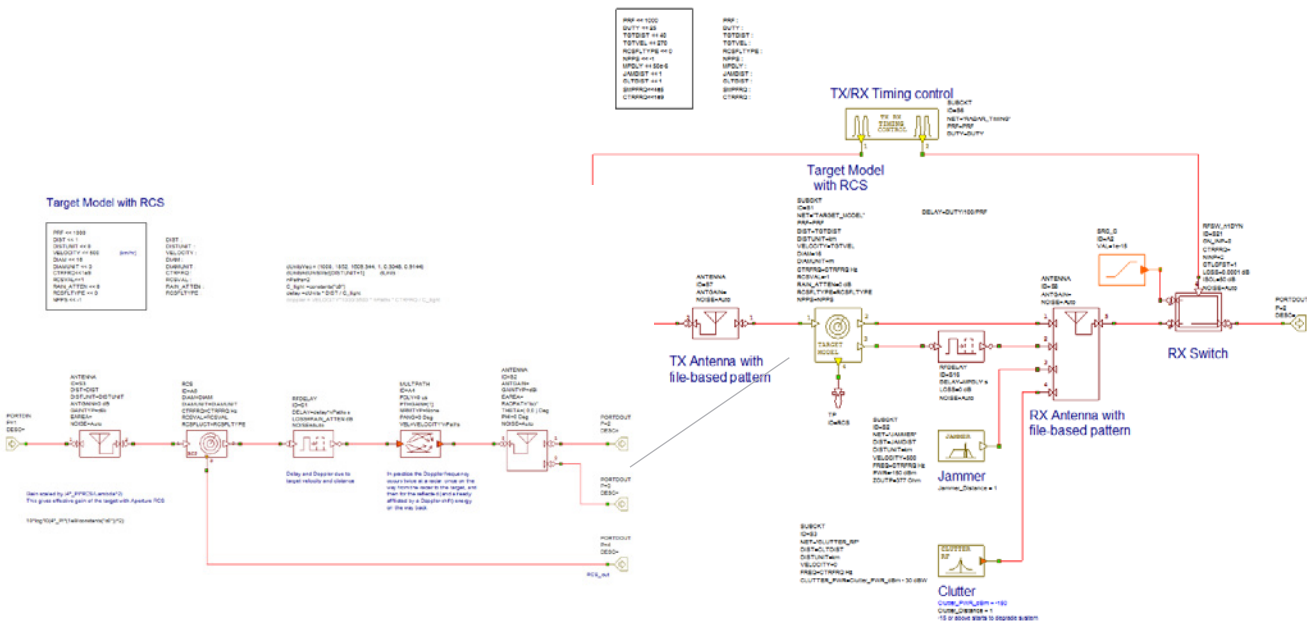


Figure 40: Subcircuit defining transmit and receive antennas, channel, and target with swept distance to radar

This relatively simple design can be used as a template for different PD applications. The radar signal is a function of pulse repetition frequency (PRF), power, and pulse width (duty cycle). These parameters can be modified for different cases. In the simulation, the radar signal also can be replaced by any defined signal through the data file reader in which the recorded or other custom data can be easily used. AWR VSS software provides the simulation and model capabilities to refine the radar architecture, implement increasingly accurate channel models (including multi-path fading and ground clutter), and develop performance specifications for the transceiver link budget and detailed antenna radiation pattern requirements.

The plots in Figure 41 show several simulation results, including the transmitted and received chirp waveform, the antenna radiation pattern, and several system measurements, including the relative velocity and distance. In this simulation, the distance to the target is swept to reflect a vehicle that approaches and passes by a stationary radar, resulting in Doppler frequency that reverses the sign from negative to positive (red curve) and produces a null in the relative distance as the target passes by the radar. In an automotive radar for ACC, the velocity and distance information would be used to alert the driver or take corrective action (such as applying the brake).

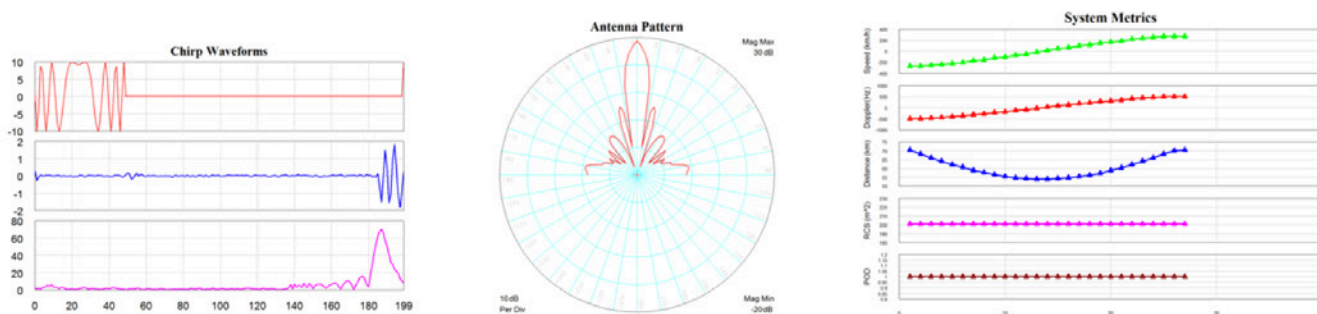


Figure 41: Results of the simulation are shown in the system metrics graph

### Multi-Beam/Multi-Range Design

A typical ACC stop-and-go system requires multiple short and long-range radar sensors to detect nearby vehicles. The shorter-range radar typically covers up to 60m with an angle coverage up to  $\pm 45^\circ$ , allowing the detection of the vehicle's adjacent lanes that may cut into the current travel lane. The longer-range radar provides coverage up to 250m and an angle of  $\pm 5^\circ$  to  $\pm 10^\circ$  to detect vehicles in the same lane, further ahead.

To support multiple ranges and scan angles, module manufacturers such as Bosch, DENSO, and Delphi have developed and integrated multi-range, multi-detection functionality into increasingly capable and cost-sensitive sensors using the multi-channel transmitter (TX)/receiver (RX) architectures, as shown in Figure 42. These different ranges can be addressed with multi-beam/multi-range radar by employing radar technology such as FMCW and digital beamforming with antenna array design.

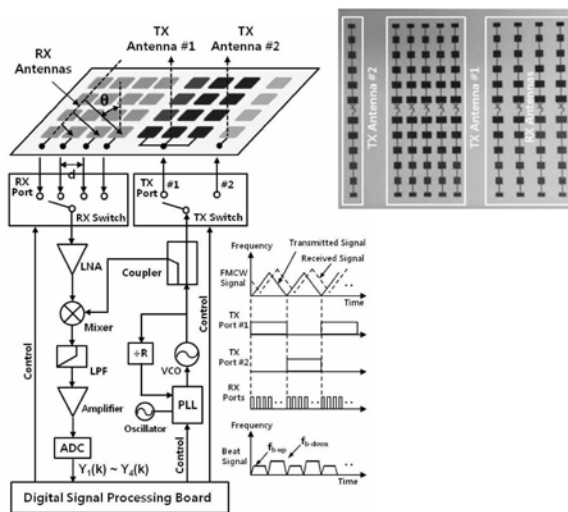


Figure 42: Multi-band, multi-range FMCW digital beam-forming ACC radar

## Antenna Design

A multi-modal radar for an ACC system<sup>2</sup> based on an FMCW radar driving multiple antenna arrays is shown in Figure 42. This multi-beam, multi-range radar with digital beamforming operates at both 24 and 77GHz, utilizing two switching-array antennas to enable long-range and narrow-angle coverage (150 m,  $\pm 10^\circ$ ) and short-range and wide-angle coverage (60 m,  $\pm 30^\circ$ ). This example illustrates the use of multiple antenna-array systems, including multiple (5x12 element) series-fed patch arrays (SFPAs) for long-range, narrow-angle detection (77GHz), a single SFPA (1x12 elements designed for 24GHz) for short, wide-angle detection, and four (1x12) SFPAs for the receiver that was required for this type of system.

Radar performance is greatly influenced by the antenna technology, which must consider electrical performance such as gain, beam-width, range, and physical size for the particular application. The multiple, fixed TR/RX antenna arrays in the example radar were optimized for range, angle, and sidelobe suppression. A patch antenna is relatively easy to design and manufacture and will perform quite well when configured into an array, which increases overall gain and directivity.

The performance of a rectangular patch antenna design is controlled by the length, width, dielectric height, and permittivity of the antenna. The length of the single patch controls the resonant frequency, whereas the width controls the input impedance and the radiation pattern. By increasing the width, the impedance can be reduced. However, to decrease the input impedance to 50 ohms often requires a very wide patch antenna, which takes up a lot of valuable space. Larger widths can also increase the bandwidth, as does the height of the substrate. The permittivity of the substrate controls the fringing fields with lower values, resulting in wider fringes and therefore better radiation. Decreasing the permittivity also increases the antenna's bandwidth. The efficiency is also increased with a lower value for the permittivity.

Designing a single patch antenna or array is made possible through the use of design software that utilizes EM analysis to accurately simulate and optimize performance. The AWR Design Environment platform includes AXIEM 3D planar and Analyst 3D FEM EM simulators. These simulators not only simulate antenna performance such as near and far-field radiation patterns, input impedance, and surface currents, they also co-simulate directly with AWR VSS software, automatically incorporating the antenna simulation results into the overall radar system analysis without the need to manually export/import data between EM simulator and system design tools.

Both AXIEM and Analyst simulators take the user-defined physical attributes of the antenna such as patch width and length, as well as the dielectric properties such as material and substrate height, to produce the electrical response. AXIEM simulator is ideal for patch antenna analysis (Figure 43), whereas the Analyst simulator is best suited for 3D structures such as modeling of a coaxial feed structure or finite dielectric (when proximity to the edge of a PCB would impact antenna performance).

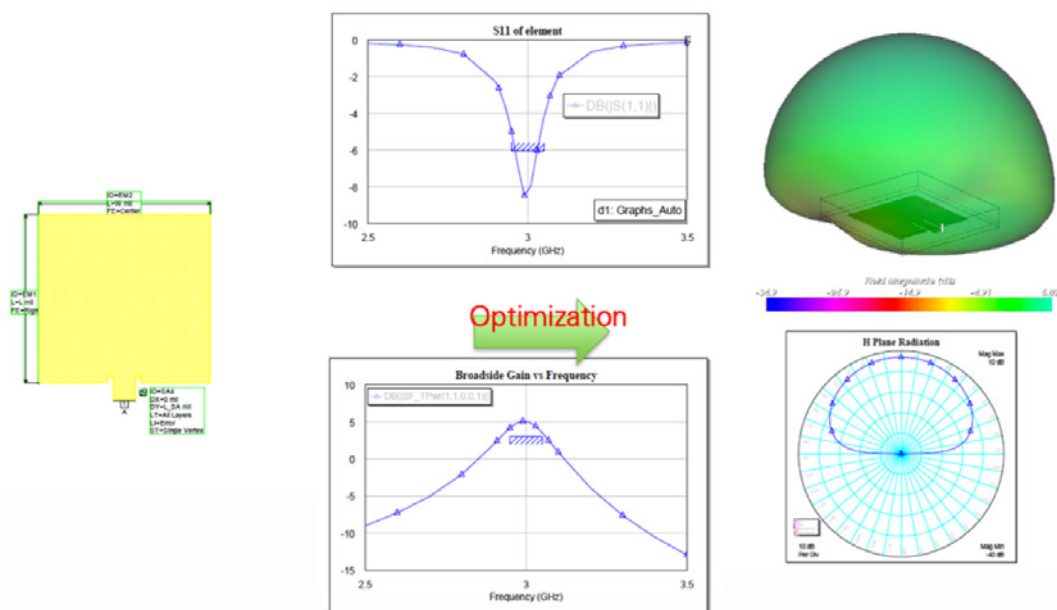


Figure 43: Edge-coupled single patch antenna optimized for center return loss and broadside gain

2. H. Jeong, H. Y. Yu, J. E. Lee, et. al., "A Multi-Beam and Multi-Range Radar with FMCW and Digital Beam-Forming for Automotive Applications," Progress in Electromagnetics Research, Vol. 124, 285-299, January 2012.

Figure 44 shows a patch antenna array with corporate feed and 167K unknowns solved in less than 6.5 minutes with a quad core.

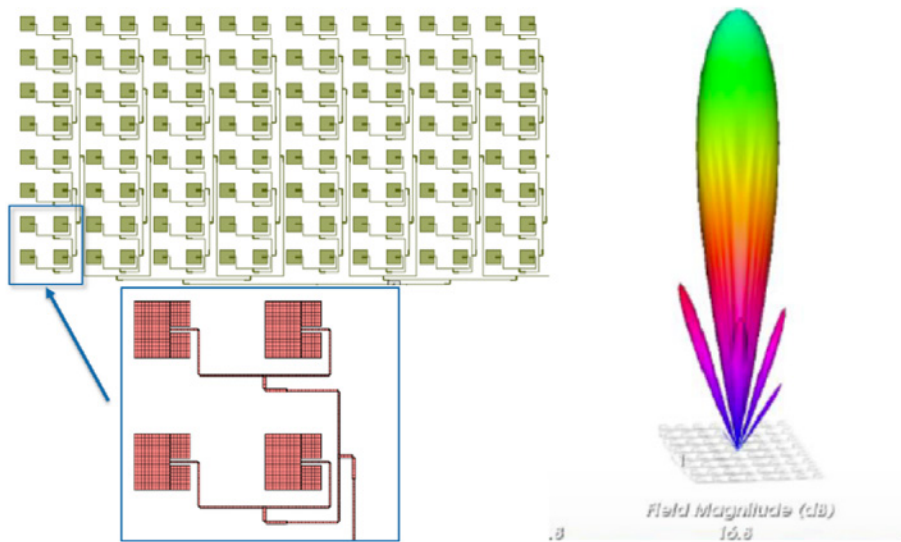


Figure 44: 8x16 patch antenna array (128-element) with corporate feed (single-feed port)

To determine the physical attributes that will yield the desired electrical response, antenna designers can use the Cadence AWR AntSyn™ antenna synthesis and an optimization module. AntSyn software enables users to specify the electrical requirements and physical size constraints of the antenna and the software explore a set of design configurations and determines the optimum structure based on proprietary genetic optimization and EM analysis. The resulting antenna geometry can then be imported in a dedicated planar or 3D EM solver such as AXIEM or Analyst simulators for verification or further analysis/optimization.

Planar elements can easily form array structures by combining very simple elements such as microstrip patches. Patches can be configured in a series such as the 1x8 patch array in Figure 45, where each element is connected serially by a “tunable” section of a transmission line. In this AXIEM project, the lengths and widths of each array element and the connecting transmission lines were defined with variables to allow optimization of the overall array performance.

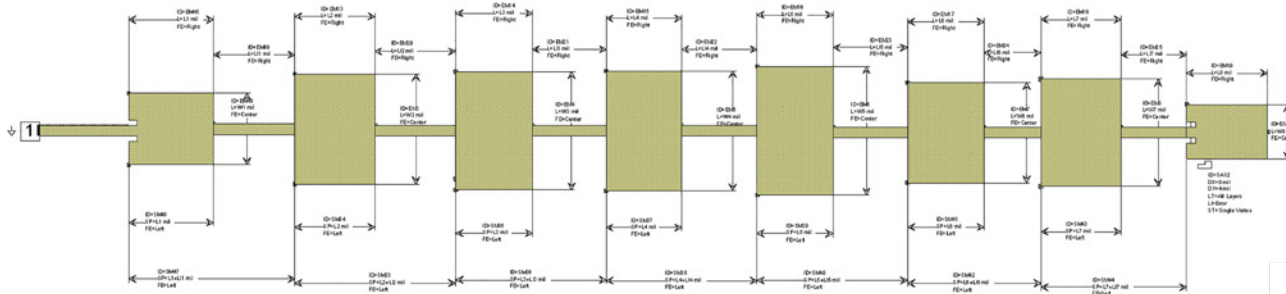


Figure 45: Series feed 1x8 patch array with parameterized modifiers

The 1x8 array can be further expanded into an 8x8 array for a high-gain fixed-beam design, as shown in Figure 46, replicating the 8x8 element array reported.<sup>3</sup>

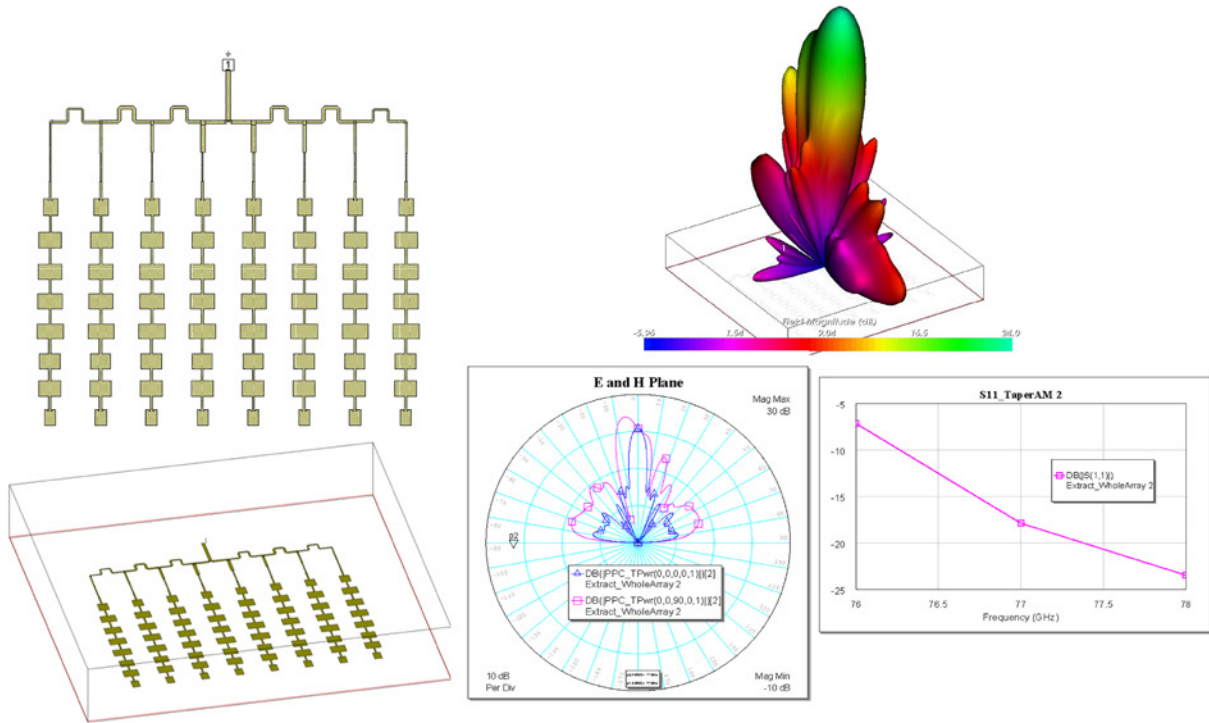


Figure 46: 77GHz 8x8 array with  $N \cdot \lambda/2$  feeding with  $\lambda/2 < \text{spacing} < \lambda$ .

Within AWR Design Environment platform, arrays can be represented in AWR VSS software as a system behavioral block using the proprietary phased-array model that enables designers to specify the array configuration (number of elements, element spacing, antenna radiation pattern, impaired elements, gain tapering, and more) for a high-level understanding of array requirements for desired performance such as gain and sidelobes. This approach is best for large-scale arrays (thousands of elements) and system designers developing basic requirements for the antenna array team.

The array can also be modeled with the detailed physical array in AXIEM or Analyst simulators. Individual port feeds can be specified or, if the feed network is also implemented in the AXIEM or Analyst simulator, a single feed network can be specified (Figure 47).

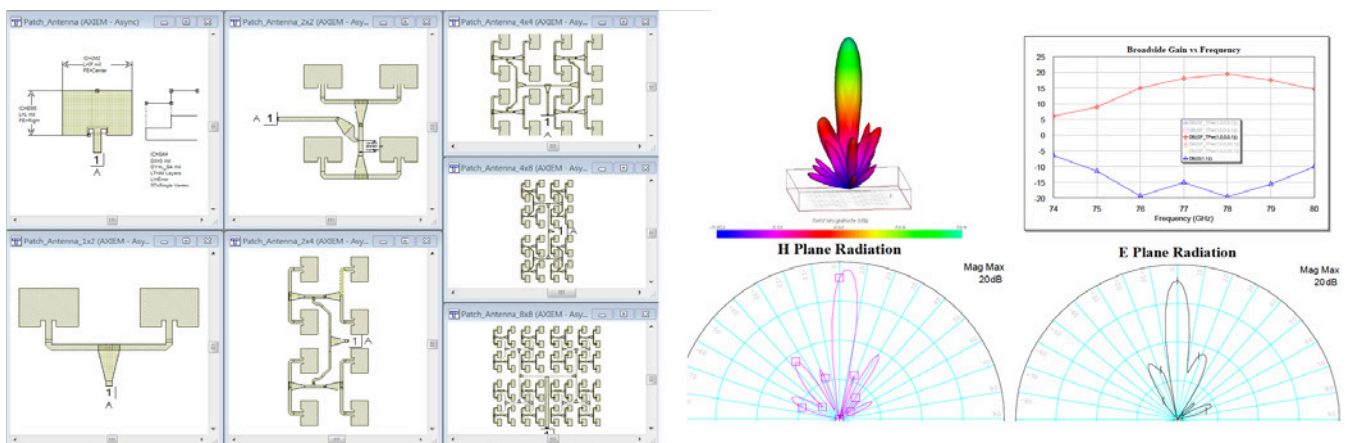


Figure 47: Simulation of published [2] 8x8 patch array on R04003C PCB, approximately 2.3x2.5cm

3. Jri Lee, Yi-An Li, Meng-Hsiung Hung, and Shih-Jou Huang, "A Fully-Integrated 77GHz FMCW Radar Transceiver in 65-nm CMOS Technology," IEEE Journal of Solid-State Circuits, Vol. 45, No. 12, December 2010.

This approach enables the design team to investigate the interaction between the beam angle and the input impedance of each element, allowing RF front-end component designers to account for impedance loading effects on transceiver performance. This capability highlights the importance of having RF circuit, system, and EM co-simulation to accurately investigate circuit/antenna behavior before fabricating these complex systems.

## MIMO and Beam-Steering Antenna Technologies

For vehicles, a radar will receive unwanted backscatter off the ground and any large stationary objects in the environment, such as the sides of buildings and guardrails. In addition to direct-path reflections, there are also multipath reflections between scatterers, which can be used to mitigate the impact of clutter through the use of multiple-input-multiple-output (MIMO) antennas.

A MIMO radar system uses a system of multiple antennas with each transmit antenna radiating an arbitrary waveform independently of the other transmitting antennas. Each receiving antenna can receive these signals. Due to the different waveforms, the echo signals can be re-assigned to the single transmitter. An antenna field of  $N$  transmitters and a field of  $K$  receivers mathematically results in a virtual field of  $K*N$  elements, resulting in an enlarged virtual aperture that allows the designer to reduce the number of necessary array elements. MIMO radar systems thereby improve spatial resolution and provide a substantially improved immunity to interference. By improving the signal-to-noise ratio, the probability of detection of the targets is also increased.

AWR VSS software is able to implement user-specified MIMO algorithms and evaluate the overall performance as it relates to the channel model, which simulates a highly-customizable multipath fading channel that includes channel path loss, the relative velocity between the transmitter and receiver, and the maximum Doppler spread. Supporting independent or continuous block-to-block operation, the channel can contain multiple paths (LOS, Rayleigh, Rician, frequency shift) that can be individually configured in terms of their fading types, delays, relative gains, and other applicable features.

This module can also simulate a receiver antenna array with user-defined geometry, enabling the simulation of single-input-multiple-output (SIMO) systems, as shown in Figure 48.

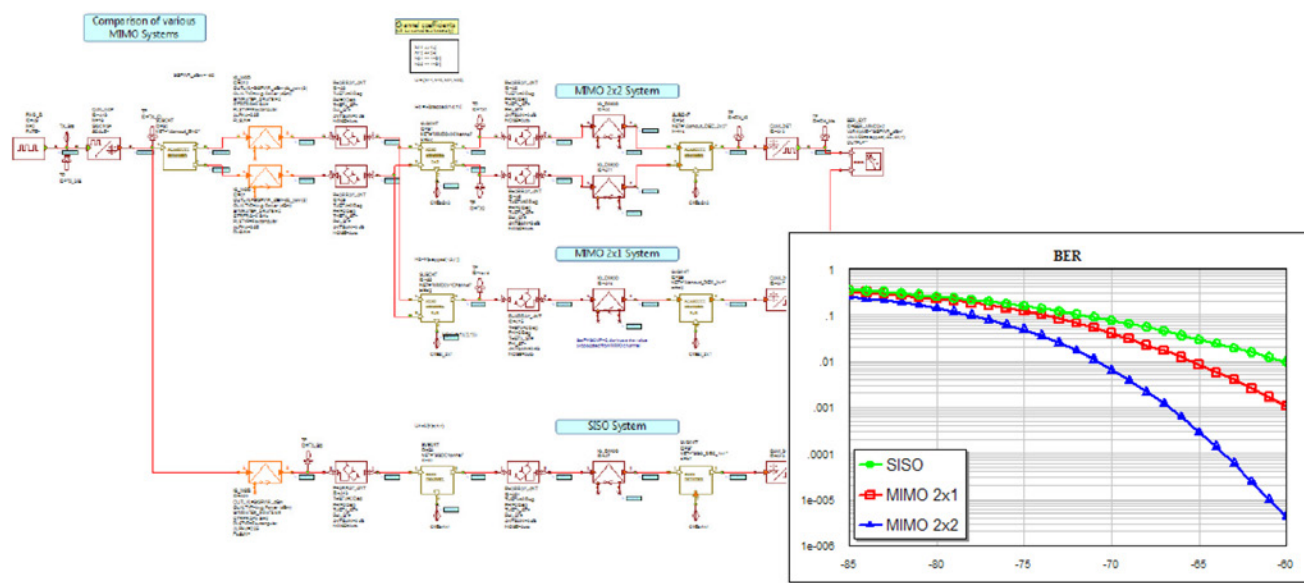


Figure 48: AWR VSS software can implement user-specified MIMO/SIMO algorithms

This application example has discussed ADAS design challenges, and examples have been presented demonstrating how the radar design capabilities within AWR VSS software help designers overcome these roadblocks. ADAS are becoming more and more prevalent in most vehicles, and continued research and development are driving more sophistication and reliability.

Advances in simulation technology like the AWR Design Environment platform, particularly in RF-aware circuit design, array modeling, and system-level co-simulation, will enable antenna designers and system integrators to optimize these systems for challenging size, cost, and reliability targets.

## MACOM Designs Ka-Band MMIC Power Amplifier (Case Study)

Ka-band technology addressing 26.5 to 40.0GHz frequencies is becoming more and more popular for both military radar and commercial communication systems, driving the need for compact, efficient power amplifiers (PAs) to boost signals for those frequencies. The practical use of load-pull tuners and electromagnetic (EM) simulation software enabled MACOM engineers to design a high-frequency, four-stage, monolithic microwave integrated circuit (MMIC) (Figure 49) that required extensive EM simulation at a relatively early stage in the design process. The characterization included S-parameter and load-pull measurements taken over wide temperature ranges using load-pull impedance tuners from Maury Microwave Corp. Measured and simulated load-pull data from AWR Design Environment simulation software was used to determine the optimum input and output impedances for the MMIC PA.

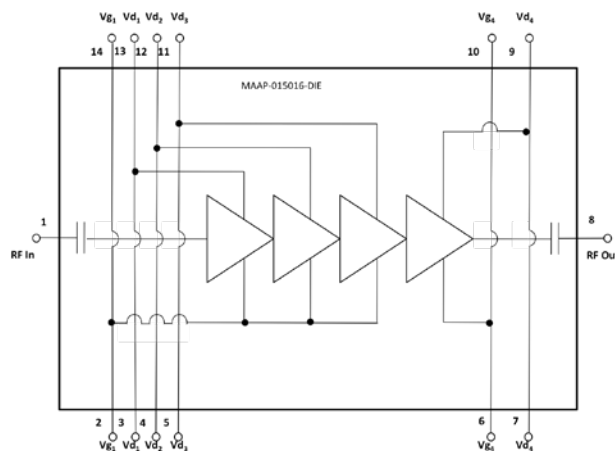


Figure 49: Block diagram of the MMIC

A large-signal simulation of an extensive array of saturated transistor cells with good convergence in a reasonable time was called for. In particular, a 3D EM simulation of the RF bond wire transition was needed (Figure 50), as well as a 2.5D (3D planar) EM simulation of the IC elements and a full large-signal simulation and optimization of the PA. Foundry models available for the 0.15  $\mu\text{m}$  GaAs process were used for the initial idealized design. Specific design requirements included a competitive size with a frequency range of 32 to 38GHz, Pout greater than 4 W, 18 dB gainfully matched to 50 ohms, continuous wave (CW) and pulsed operation, and on-chip decoupling and electrostatic discharge protection.

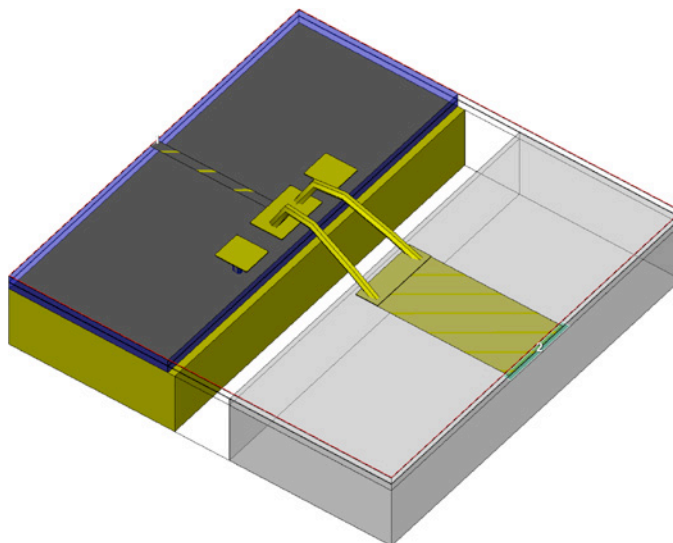


Figure 50: 3D Analyst layout view showing bond wires

MACOM designers used AWR Design Environment software, inclusive of Microwave Office circuit design software, AXIEM 3D planar EM simulator, Analyst™ 3D FEM EM simulator, and APLAC harmonic balance (HB) simulator. The software enabled them to successfully design and simulate the 4 W Ka-band PA using a 2-mil thick 0.15  $\mu\text{m}$  GaAs pseudomorphic high electron mobility transistor (pHEMT) process. Figure 51 is a photograph of the circuit, as well as the corresponding 3D meshed layout view in the AXIEM simulator for the output matching section (green traces in photo).

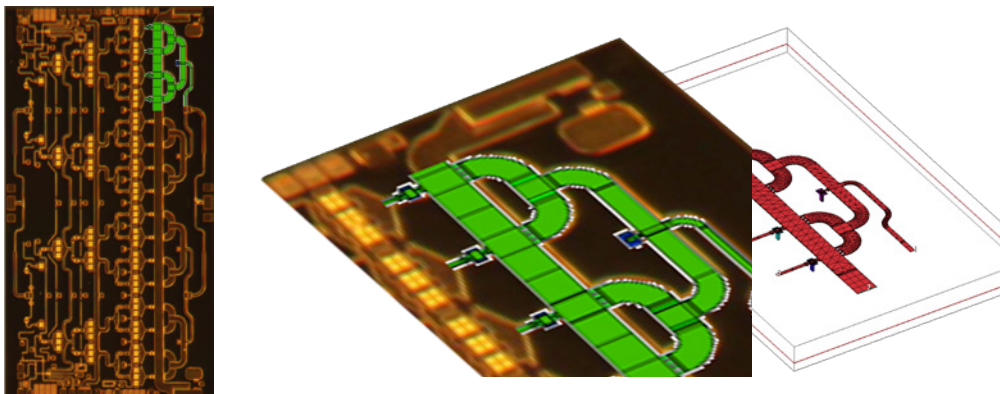


Figure 51: Photograph of the circuit as well as corresponding 3D meshed layout view of AXIEM EM simulator for the output matching section (green traces in photo)

The designers achieved saturated output power above 4W over the full 32–38GHz bandwidth, with a gain of 19 dB and power-added efficiency (PAE) in the region of 23%. A comparison of measured results with simulated performance as predicted with AWR Design Environment software (Figure 52) shows a good correlation that validates the design process. As is typical, output power performance measured slightly lower than simulation, while measured PAE is slightly better than predicted by simulation. Despite the variation in magnitude of these parameters, the similar shape of the response curves indicates that the circuit was accurately characterized in simulation.

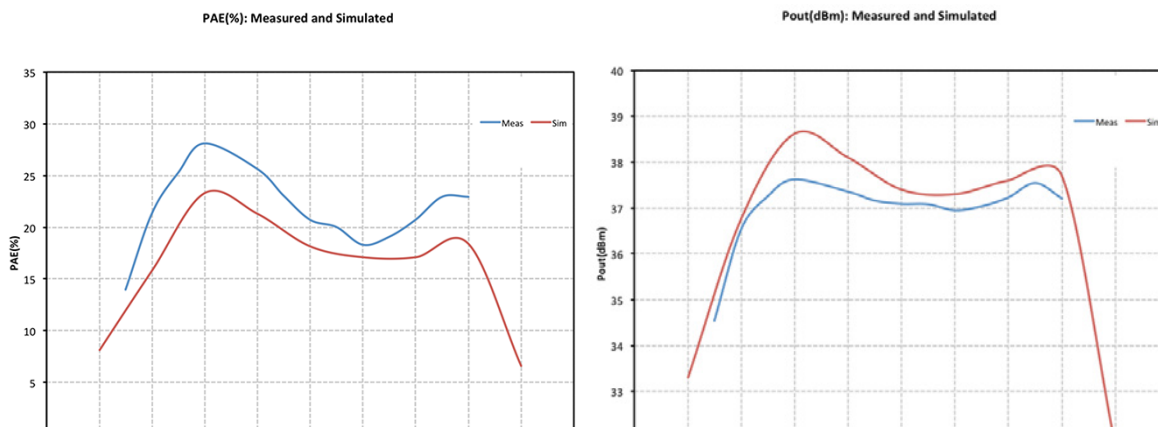


Figure 52: Measured vs. simulated results for PAE and  $P_{out}$

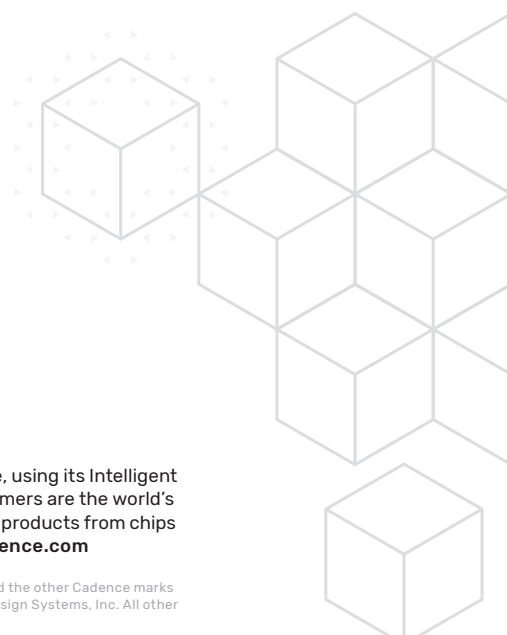
Excellent performance was verified under both CW and pulsed conditions. The results justified the design approach in terms of device modeling, circuit design, EM simulation, and even thermal considerations.

The design team noted that with AXIEM, EM simulations were quick to set up, and it was easy to adjust geometry dimensions for performance tuning. Simulation times were reasonable even when simulating from a laptop. Integration with the layout through AWR Design Environment software ensured consistency between EM and layout. The APLAC HB engine was fully capable of handling large transistor array simulations with good convergence across the band. The team was especially impressed with the ease of management of the entire design project from measured cell data, EM designs, layout, and reticle design, through to exporting graphs and graphics for reporting.

The MACOM designers chose AWR software because of their familiarity with the tool and its intuitive user interface including a high-quality layout. The key benefit was an excellent correlation between the simulations and measurements. AWR Design Environment delivered higher productivity thanks to its ease of use, integration with third-party tools, and superior technical support.

## Conclusion

Radar technology, driven by new commercial and aerospace/defense applications, is enabled by evolving semiconductor, phased array, and integration technologies. EDA simulation software provides the necessary support for engineers developing the hardware responsible for these data-intensive, wireless sensors. As the underlying RF front-end technology and digital signal processing continue to grow more complex, RF-aware system simulation, inclusive of nonlinear RF circuit and EM antenna analysis, plays a critical role in the physical realization of these beam-steering and MIMO-based radar systems. AWR software includes all of the modeling and simulation technologies designers need to meet the challenges of all types of radar system design. To learn more about the breadth of products available for radar design, visit [awr.com/radar](http://awr.com/radar).



**cādence**<sup>®</sup>

Cadence is a pivotal leader in electronic design and computational expertise, using its Intelligent System Design strategy to turn design concepts into reality. Cadence customers are the world's most creative and innovative companies, delivering extraordinary electronic products from chips to boards to systems for the most dynamic market applications. [www.cadence.com](http://www.cadence.com)

© 2020 Cadence Design Systems, Inc. All rights reserved worldwide. Cadence, the Cadence logo, and the other Cadence marks found at [www.cadence.com/go/trademarks](http://www.cadence.com/go/trademarks) are trademarks or registered trademarks of Cadence Design Systems, Inc. All other trademarks are the property of their respective owners. 15591 12/20 DB/RL/WP-RDR-SYS/PDF